Diana Marisa Marques dos Santos

Degree in Biochemistry

Improving a bacterial pyranose 2-oxidase from *Arthrobacter siccitolerans* through directed evolution

Dissertation to obtain the Master Degree in Biochemistry for Health

Supervisor: Lígia O. Martins, PhD, ITQB-UNL

October 2017

Diana Marisa Marques dos Santos

Degree in Biochemistry

Improving a bacterial pyranose 2-oxidase from *Arthrobacter siccitolerans* through directed evolution

Dissertation to obtain the Master Degree in Biochemistry for Health

Supervisor: Lígia O. Martins, PhD, ITQB-UNL

Júri:

Presidente: Prof. Doutor Pedro Matias

Arguente: Prof. Doutora Manuela M. Pereira

Vogal: Doutora Margarida Archer

Instituto de Tecnologia Química e Biológica António Xavier

October 2017

Improving a bacterial pyranose 2-oxidase from *Arthrobacter siccitolerans* through directed evolution

Acknowledgments

Nesta fase final da minha dissertação de mestrado, gostaria de demonstrar a imensa gratidão com todas as pessoas que me apoiaram e que contribuíram ao longo do último ano para a minha formação como pessoa e investigadora. Não poderia deixar de agradecer a todo o ITQB, especialmente ao laboratório MET por me fornecerem todas as condições e equipamentos sem os quais não poderia ter elaborado esta dissertação.

Vou ficar eternamente grata à minha orientadora: professora Lígia Martins por todo o apoio e transmissão de conhecimento que me facultou! Um obrigada nunca vai ser suficiente por nunca me deixar desanimar quando as coisas não corriam da forma desejada, por me fazer acreditar na ciência, por ter sempre total disponibilidade para me ajudar mesmo quando o tempo era escasso e por me encorajar a lutar pelos meus objetivos todos os dias com otimismo. Terei sempre uma grande admiração pela grande cientista que é mas também pela excelente pessoa que demonstra todos os dias ser. Sem dúvida, um exemplo a seguir!

Não poderia deixar de agradecer à Dra. Vânia Brissos que tanto me ajudou ao longo de toda a minha dissertação de mestrado. Sempre com total disponibilidade para me esclarecer todas as dúvidas e fornecer valiosos conselhos que a vasta experiência lhe ensinou e que com todo o gosto me transmitiu. Obrigada pelo tempo, todo o conhecimento e ajuda que disponibilizou e que tanto me foram úteis.

Quero ainda agradecer à Dra. Sónia Mendes, pela energia positiva que sem dúvida contagia as pessoas ao redor e pela ajuda que sempre me foi disponibilizada. Aos membros do MET que ao longo deste ano estiveram presentes no laboratório (Patrícia, Ana, Manuel, Lorenzo e Diogo) um obrigada pelos bons momentos passados e por tornarem por vezes momentos de stress em momentos divertidos.

Gostaria ainda de agradecer à Dra. Mónica Serrano pela ajuda e disponibilidade que demonstrou ter quando necessitei de utilizar a técnica de microscopia de fluorescência e ao professor Willem van Berkel e Dr. Adrie Westphal (Univ. Wageningen, Holanda) pelo modelo da proteína que construíram.

Aos meus pais, por serem o meu refúgio quando atravesso momentos menos bons, pelo trabalho constante que desenvolvem todos os dias para me proporcionarem a oportunidade de tirar um curso superior, de seguir sempre os meus sonhos e concretizar os meus objetivos. Nunca haverá palavras suficientes para agradecer todo o apoio incondicional e motivação que me transmitiram não só durante esta fase mas sim durante toda a minha vida.

Ao meu namorado e acima de tudo melhor amigo Daniel, obrigada por todo o apoio durante esta fase, por nunca me deixar desmotivar e pela compreensão quando nem sempre lhe conseguia dar a atenção devida. Da mesma forma, um obrigada a todos os meus amigos por sempre me apoiarem, acreditarem em mim e compreenderem quando nem sempre podia despender o tempo devido com eles.

Resumo

Piranose 2-oxidases (P2Ox) são flavoproteínas que catalisam a oxidação do carbono 2 de aldopiranoses, com redução concomitante de O_2 a H_2O_2 e, que apresentam, um grande interesse biotecnológico. Recentemente, foi caracterizada pela primeira vez, uma P2Ox bacteriana, AsP2Ox de *Arthrobacter siccitolerans*. As bactérias apresentam maior rapidez de crescimento, em comparação com os fungos, e existe grande disponibilidade de ferramentas de biologia molecular em sistemas bacterianos. No entanto, verificou-se que a eficiência catalítica de AsP2Ox era seis-ordens de magnitude inferior à exibida pelas enzimas fúngicas. Neste trabalho, a evolução dirigida foi utilizada na engenharia da enzima AsP2Ox, para melhoramento da sua eficiência catalítica. Otimizaram-se protocolos de mutagénese, seleção e crescimento de células hospedeiras, lise celular e ensaios enzimáticos. A aplicação de uma estratégia validada de mutagénese e "screening" permitiu a seleção de um variante, 2C9, com atividade enzimática superior à observada na enzima nativa, a partir de uma biblioteca de 25 000 clones. Após purificação, verificou-se que o seu nível de produção era 6 vezes mais baixo relativamente à enzima nativa e mostrava ser inativado pela luz. Este variante contém duas mutações não sinónimas (A35T e F300V) e uma sinónima (Q343Q). Com o objetivo de avaliar o efeito das mutações nas propriedades do variante, foram construídos os mutantes "single" (A35T e F300V) e o mutante duplo 2C9* (A35T/F300V), sem a mutação sinónima. Concluiu-se que a mutação Q343Q era a única responsável pela foto-inativação da enzima, e, em conjunto com a mutação F300V, contribuía para os níveis de produção mais baixos. Verificou-se ainda que a mutação A35T era neutra, mas indispensável para, combinada com a mutação F300V, numa interação epistática, resultar numa eficiência catalítica 3 vezes superior no variante 2C9*, relativamente à enzima nativa. Assim sendo, o mutante 2C9* foi selecionado como parente para uma segunda geração de evolução dirigida.

Palavras-chave: flavoproteínas, enzimas formadoras de peróxido, evolução dirigida, eficiência catalítica, biosensores

Abstract

Pyranose 2-oxidases (P2Ox) are flavoproteins that catalyze the oxidation of several aldopyranoses to yield the corresponding 2-keto-aldoses with concomitant reduction of O_2 to H_2O_2 and are enzymes that show many biotechnological applications. Recently, a bacterial P2Ox from *Arthrobacter siccitolerans* (AsP2Ox) was characterized for the first time since bacteria grow faster as compared to fungi and have well-established genetic and molecular biological tools allowing for higher enzyme production yields. Directed evolution has proven to be a powerful approach to improve enzyme efficiency and robustness required for biotechnological applications. Therefore, in this work the optimization and validation of critical steps of directed evolution was performed, namely mutagenesis protocols, cell growth, lysis and high-throughput enzymatic assays. One round of evolution through error prone PCR was performed and a total of 25 000 clones were screened to find variants with improved activity for D-glucose and dioxygen. One hit variant, 2C9, was identified, showing higher activity than wild-type and containing two non-synonymous (A35T and F300V) and one synonymous mutation (Q343Q). The variant enzyme was produced at a larger scale, purified and characterized. It was observed that 2C9 was produced at 6-fold lower yields as compared to wild-type and showed photo-inactivation behaviour. Therefore single mutants (A35T and F300V) and double 2C9* without the silent mutation (A35T/F300V) were constructed and characterized to unveil the role of mutations from the catalytic and structural viewpoints. The introduction of the synonymous mutation Q343Q resulted in the photo-inactivation of the enzyme and was co-responsible, along with the F300V mutation, to the variant lower production yields. Mutation A35T was neutral but in combination with the functional F300V mutation, an epistatic effect became evident, resulting in the 3-fold higher catalytic efficiency exhibited by 2C9* as compared with the wild-type enzyme. Therefore, 2C9* was selected as a parent for the second generation of directed evolution.

Keywords: flavoproteins, hydrogen peroxide forming enzymes, directed evolution, catalytic efficiency, biosensors

Table of contents

List of Figures

List of tables

List of Abbreviations

1,4-BQ - 1,4-benzoquinone

1,5-AG - 1,5-anhydro-D-glucitol

ABTS - 2,2'-azino-bis (3- ethylbenzothiazoline-6-sulfonic acid)

BLAST - Basic Local Alignment Search Tool

B-PER - Bacterial Protein Extraction Reagent

APS - Ammonium persulfate

AsP2Ox - Pyranose 2-oxidase from *Arthrobacter siccitolerans*

BSA - Bovine Serum Albumin

DCPIP - 2,6-Dichlorophenolindophenol

epPCR - Error prone polymerase chain reaction

FACS - Fluorescence-activated cell sorting

FAD - Flavin adenine dinucleotide

GMC- Glucose-methanol-choline

GOx - Glucose oxidase

HRP - Horseradish peroxidase

IPTG - Isopropyl β-D-1-thiogalactopyranoside

kDa - Kilodalton

LB – Luria-Bertani

OD_{600nm} - Optical density at 600 nm

P2Ox - Pyranose 2-oxidase

PCR - Polymerase chain reaction

RT - Room temperature

SDS-PAGE - Sodium dodecyl sulfate polyacrylamide gel electrophoresis

SOB - Super Optimal Broth

SDM – Site-directed mutagenesis

SSM - Site-saturation mutagenesis

TB - Terrific Broth

TCA - Trichloroacetic acid

TEMED - N, N, N', N'-Tetramethylethylenediamine

Tris – Tris (hydroxymethyl)aminomethane

UV-Vis - Ultraviolet-Visible

1. Introduction

1.1. Fungal pyranose oxidases: General properties and catalysis

Pyranose 2-oxidases (P2Ox, pyranose: oxygen 2-oxidoreductase; EC 1.1.3.10; synonym, glucose 2-oxidase) belong to the glucose-methanol-choline (GMC) oxidoreductase superfamily of enzymes[1]. This family includes enzymes such as glucose oxidase, choline oxidase, cholesterol oxidase, cellobiose dehydrogenase, aryl-alcohol oxidase, pyridoxine 4-oxidase, among others[1]. P2Oxs are flavin adenine dinucleotide (FAD)-dependent enzymes, exhibiting the typical UV–Visible spectrum of the FAD cofactor with absorption maxima at 360 and 455 nm[2].

P2Oxs catalyze the regiospecific oxidation of sugar molecules at an alcohol moiety (-CH-OH) to the corresponding aldehyde with concomitant reduction of molecular oxygen to hydrogen peroxide[3,4]. Several aldopyranoses and disaccharides such as D-glucose, D-galactose, D-mannose, D-arabinose, D-fructose, L-sorbose, D-xylose, D-fucose, maltose and trehalose are oxidized at the C2 position to yield the corresponding 2-keto-aldoses[5,6]. These enzymes can also use quinones as electron acceptors in replacement to O_2 and show a higher efficiency for substituted benzoquinones, structural analogues of benzoquinone (*e.g.* DCPIP), metal ions such as ferricyanide and ferrocenium, and radicals (*e.g.* the cation radical $ABTS^{\bullet+}$)[7]. The specific activity of P2Ox for the different sugar substrates varies considerably, but D-glucose has been identified as the favourite substrate[4]. Oxidation at the C3 position, as a side reaction, was also observed with 2-deoxy-D-glucose, 2-keto-D-glucose and methyl β-D-glucosides, indicating that when the C2 hydroxyl group is compromised, P2Oxs have the ability to oxidize sugar substrates at a different position, demonstrating an alternative regioselectivity[8,9,10].

The first P2Ox enzyme was isolated from the fungus *Polyporus obtusus*, followed by its characterization in several other P2Oxs, mainly from wood-degrading, white- and brown-rot, basidiomycetes[11]. In these microorganisms, P2Oxs are located in the hyphal periplasmic space and are released to the extracellular space in the later stages of the fungal cycle development[11]. Fungal enzymes have D-glucose, D-galactose and D-xylose as preferred substrates most likely due to their abundance in lignocellulose material originated from wood rot. Their physiological role has been associated with the generation of H_2O_2 that is an essential substrate for lignin-degrading peroxidases[5,12]. Furthermore, it was shown that in some species of white-rot fungi, P2Oxs are involved in secondary metabolic pathways that lead to the production of the antibiotic cortalcerone, protecting the microorganism from bacterial attack[5]. As quinones act as alternative electron acceptors to O_2, it has been claimed that P2Oxs can also get involved in the reduction of quinones during the process of ligninolysis[11].

The reaction catalyzed by P2Oxs can be divided in two half-reactions: a reductive half-reaction, where the transfer of two electrons from a sugar substrate to the oxidized FAD occurs leading to the formation of a 2-keto-sugar and reduced $FADH_2$, and an oxidative half reaction, where two electrons from the reduced $FADH_2$, are transferred to molecular oxygen, with concomitant formation of H_2O_2[3,13] (figure 1.1). The first evidence for the formation of an intermediate in a flavoprotein oxidase was detected in P2Ox, the C-4a-hydroperoxyflavin intermediate, observed during the oxidative half reaction, when O_2 acts as electron acceptor[11]. Considering that the 2-keto-sugar product is thought to be released before oxygen

reduction, the mechanism of the reaction catalyzed by P2Oxs was classified as a ping-pong bi-bi type, characteristic of flavoprotein oxidoreductases[1]. Typically, P2Oxs activity is measured through H_2O_2 production in a coupled spectrophotometric assay using a commercial peroxidase and a chromogen substrate, or using an O_2 electrode by measuring the rate of O_2 consumption[2].

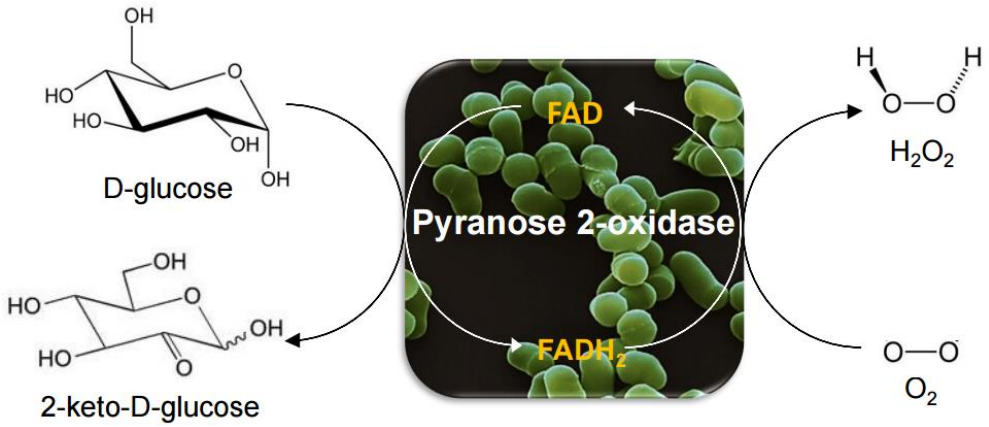

Figure 1.1 Schematic reaction catalyzed by P2Ox: first the transfer of two electrons from D-glucose to the FAD cofactor occurs followed by O_2 reduction resulting in the formation of 2-keto-D-glucose and H_2O_2.

1.2. Pyranose 2-oxidase from *Arthrobacter siccitolerans* (AsP2Ox)

P2Oxs from fungal origin have been extensively studied and characterized. Consequently, in our lab it was settled as an objective to isolate and characterize a P2Ox enzyme from bacterial origin: *Arthrobacter siccitolerans* (AsP2Ox). In these microorganisms, recombinant proteins are easier and cheaper to produce, since they reach higher cell densities in shorter periods of time as compared with fungi, and there are plenty of genetic and molecular tools available[14]. A bioinformatics analysis was performed using Basic Local Alignment Search Tool (BLAST) in all bacterial genomes available using as template the sequence of the fungal P2Ox from *Trametes multicolor*. The top 100 Blast sequence hits from bacterial genomes showed an identity between 24 and 39% to the template and 85 out of 100 sequences identified belong to members of the *Actinobacteria*[3] phyla, one of the most dominant in the bacteria domain, present in varied ecosystems such as alkaline saline soils, marine sponges, deep sea sediments, hot springs, gut and medicinal plants. *Actinobacteria* displays an important biological role in biogeochemical cycles, bioremediation, bioweathering and plant growth promotion[15,16]. Furthermore, they produce a large number of pharmaceutically bioactive compounds such as antibiotics, antitumor agents, anti-inflammatory compounds, enzyme inhibitors and a wide variety of industrial and clinically important enzymes[16]. The most represented putative P2Ox sequences (62%) are from species of the *Streptomyces* (14), *Arthrobacter* (17) and *Microbacterium* (25) genera. The *A. siccitolerans* genome revealed an ORF encoding a 519 amino acid polypeptide that showed 26% homology with the P2Ox template sharing 13 of the 15 strictly conserved residues present in GMC family in the: (i) FAD-binding domain, (ii) flavin attachment loop and (iii) substrate binding domain that was putatively assigned as a

pyranose 2-oxidase (AsP2Ox)[3,17,18]. The gene was cloned and the enzyme was overproduced in *Escherichia coli*. After purification, AsP2Ox showed a yellow colour and the typical flavoprotein visible absorption spectrum with two peaks at 390 and 460 nm, with a flavin-protein molar ratio of approximately 1:1[3]. Unlike most known fungal enzymes, in AsP2Ox, the FAD molecule is not covalently bonded to the protein and the enzyme is monomeric with a molecular mass of 64 kDa, while fungal counterparts are tetrameric enzymes. AsP2Ox exhibited an optimal temperature at 37ºC, an optimum pH of 6.5 and oxidizes D-glucose at the highest efficiency, using additionally D-galactose, D-xylose, L-arabinose and D-ribose as electron donors, coupling their oxidation to the reduction of both dioxygen and 1,4-benzoquinone (1,4-BQ), the preferred electron acceptor[3]. It shows a K_m value 2-orders of magnitude higher and a k_{cat} between 2 to 3 orders of magnitude lower for D-glucose and dioxygen when compared with P2Ox characterized from fungal origins resulting in a 6 to 7-orders of magnitude reduced catalytic efficiency (k_{cat}/K_m)[11,12].

1.3. Structural characterization of P2Ox

Only three crystal structures were reported to date for P2Oxs from fungal origin: *T. multicolor*[19], *Peniophora sp.*[20] and *Phanerochaete chrysosporium*[10]. All structures are homotetrameric proteins, in some cases glycosylated, constituted by a dimer of dimers with molecular masses in the range of 280-320 kDa[2] (figure 1.2-A). FAD is covalently linked to the monomers by a histidyl linkage[21]. As shown in figure 1.2-B, each subunit of the homotetramer can be seen as a central, peanut-shaped elongated 'body' with an 'arm' projected to the outside that is responsible for the contact with neighbouring subunits and a 'head' (αββα motif) that possibly acts as a immobilizer of the enzyme in the fungal cell-wall[19]. The FAD-subdomain presents a Rossman fold (βαβ mononucleotide-binding motif) and the substrate-binding subdomain is composed by a central six-stranded β sheet packed between the active site and three α helices[19].

The substrate has to pass through a large, internal cavity that contains water, before accessing the active site of each subunit[19]. The amino acid residues with a role in the catalytic reaction of *T. multicolor*, and that are conserved in other fungal P2Oxs, are His548, Asn593, Gln448, His450 and Val546. With the support of Asn593, the His548 amino acid residue most probably acts as a base and deprotonates the substrate at the 2-OH group with a subsequent hydride transference to the flavin N(5) atom[19]. In AsP2Ox, the main catalytic amino acid residues (His440, Asn484 and Gln340) are conserved, however catalytic residue His450 in *T. multicolor* P2Ox appears as Met342 in AsP2Ox and Val546 in *T. multicolor* P2Ox as Ser438 in AsP2Ox, which can have implications in the catalytic reaction.

The active site of *T. multicolor* P2Ox is gated by a dynamic, highly conserved loop (residues 450-461) that presents several residues that efficiently bind both electron-donor (sugar) and electron-acceptor substrates (oxygen or quinone derivates) and are therefore determinant for the substrate binding and catalysis[19,22]. Through the analyses of two P2Ox crystal structures, one in a sugar free form (acetate-bonded, figure 1.2-C) in native P2Ox and the other in a sugar-bonded form (2-keto-D-glucose-bonded, figure 1.2-D) in the mutant H167A enzyme, it is possible to observe at least two loop conformations that were assigned to the two half-reactions of the enzyme[19].

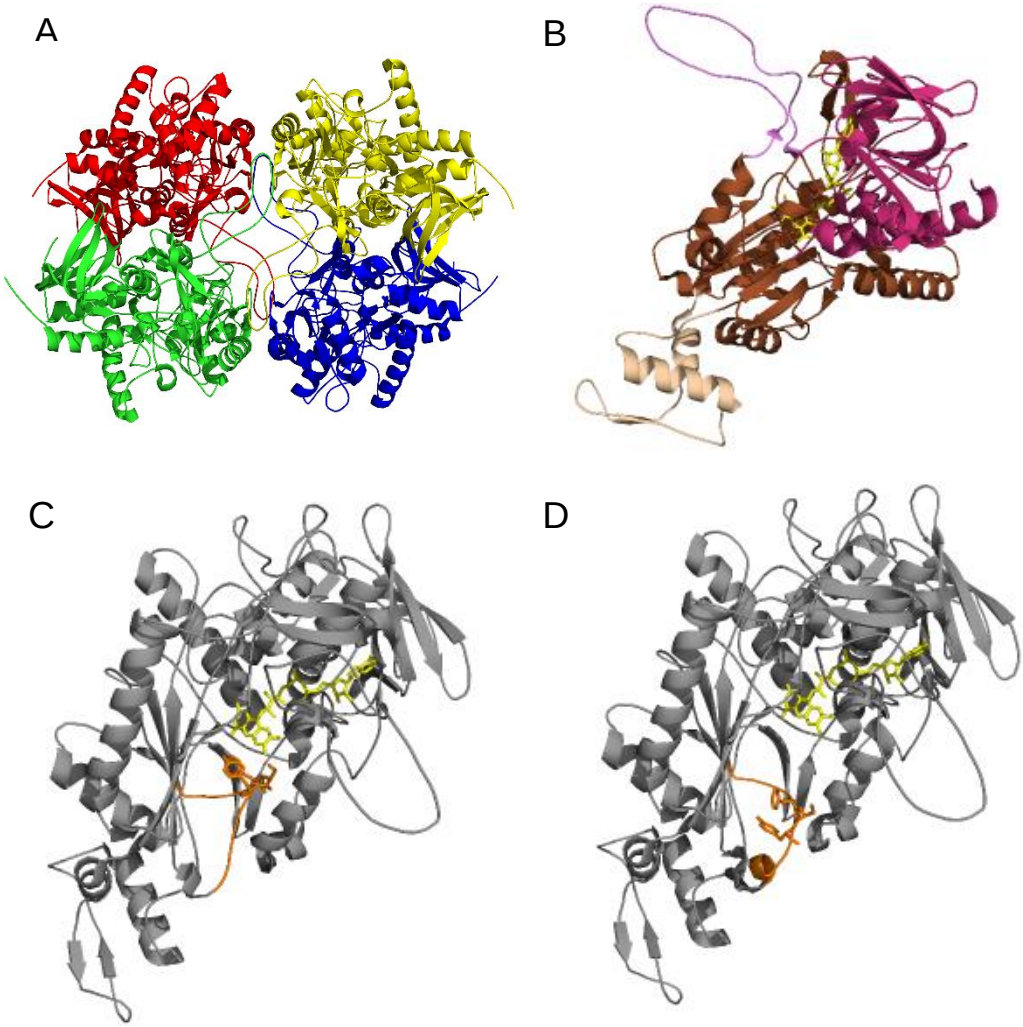

Figure 1.2 Crystal structure of P2Ox from *T. multicolor*[19]. (A) Homotetramer structure and subunit assembly. (B) Structure of P2Ox subunit. In purple is represented the oligomerization arm and in beige the head domain. The Rossman domain is represented in pink and the substrate binding domain in brown. The FAD cofactor is shown as a yellow stick representation. Subunit structure with the substrate-recognition loop represented in orange in a closed (C) and open (D) conformation. The gating segment (Phe[454], Ser[455] and Tyr[456]) is shown as an orange and FAD cofactor as a yellow stick representation in (C) and (D). (A), (B), (C) structures corresponds to PDB code 1TT0 and (D) to PDB code 2IGO.

When the P2Ox enzyme is in complex with small ligands (*e.g.* acetate), the loop is in a fully closed conformation with the active site less accessible, providing a more hydrophobic environment, appropriate for the reaction of the reduced enzyme with electron-acceptors such as dioxygen, and for the accommodation and stabilization of the C(4a)-hydroperoxyflavin intermediate, during the oxidative half-reaction (figure 1.2-C)[19,23,24]. The structure of the H167A mutant shows that the loop is in an open conformation, suitable to accommodate the sugar substrates in the reductive half-reaction (figure 1.2-D)[9,22]. The observed conformational transition is apparently due to the [454]FSY[456] motif in the substrate-recognition loop, which, in the oxidative half-reaction, comes closer to the active site, blocking access of larger substrates, such as sugars[22]. It was demonstrated that these residues are intolerant to substitution, but in AsP2Ox only the serine residue is conserved, [346]ASP[348], with structural and functional

consequences that are yet to be understood. Among members of the GMC family of enzymes with three-dimensional structures available, only P2Oxs present a covalently bonded FAD which is recognized to facilitate the substrate oxidation and help to increase the redox potential of the enzyme[19,25]. The sequence motif associated with flavinylation of the P2Ox is ^{165}STHW^{16819} and in AsP2Ox, the corresponding motif has two alanine residues that are not conserved: ^{125}AAHW^{128}. As previously mentioned, AsP2Ox does not present a covalently bonded FAD cofactor, which can relate to the alteration of this motif despite its absence apparently not affects the redox potential of the enzyme (-50 mV) that is slightly higher that the fungal counterpart with known redox potential (-105 mV)[1].

1.4. Applications of P2Oxs

In the last decades there has been an increased interest in the use of P2Oxs as a biocatalyst for the construction of biosensors or biofuel cells by biotechnological industries. P2Ox has the potential to substitute the widely used glucose oxidase (GOx) as an analytical reagent in diagnostic kits. The main advantages of P2Ox in relation to GOx are the high range of substrates and the lack of an anomer preference (GOx only oxidizes the β-anomer of D-glucose), which leads to an improvement in the response time of the reaction[2,26].

P2Oxs can be used in biosensors and biofuel cells through the utilization of redox mediators such as osmium, redox polymers, ferrocenes or benzoquinone that have the ability of transfer electrons from the enzyme to the electrode[11]. The number of diabetic patients is increasing nowadays and it is possible to employ P2Oxs in biosensors constructed for the determination of 1,5-anhydro-D-glucitol (1,5-AG), a natural analogue of D-glucose present in human cerebrospinal fluid and in serum[2,27]. It is known that a decrease of this compound in serum is related with hyperglycemia or renal dysfunction and therefore P2Ox can be used as a marker of glycemic control in diabetes mellitus[2,28]. A commercial biosensor with P2Ox (GlycoMark) based at H_2O_2 measurement is currently in the market and other detection methods are being tested using, for example, electrochemical impedance spectroscopy[29,27]. Recently, P2Ox was immobilized and stabilized in carbon nanotubes, to improve the glucose sensitivity of biosensors and to increase the power density of biofuel cells. When tested in the determination of sugars in soft drinks, P2Ox showed a higher sensitivity compared to the GOx enzyme[30,31].

Another potential application of P2Ox is in carbohydrate chemistry for the development of efficient routes that convert bulk carbohydrates into more valuable products and materials[32,33]. This application relies on the large number of products with industrial interest that can be produced using 2-keto-D-glucose as intermediate: D-fructose, mannitol, 2,3-di-keto-4-deoxy-D-glucose, that are part of the pathway for the production of rare sugars, fine chemicals and drugs[32]. One example of a drug produced from 2-keto-D-glucose is the β-pyrone antibiotic cortalcerone[34]. This antibiotic is rare in nature and can be produced using two enzymatic steps: D-glucose is first oxidized to 2-keto-D-glucose by P2Ox which is then dehydrated to cortalcerone by pyranosone dehydratase[35,36]. In addition to 2-keto-D-glucose, other keto-sugars can be produced using P2Ox, including 2-keto-D-galactose, a precursor of the rare sugar D-tagatose, a low-calorie and noncariogenic sweetener, and 2-deoxy-3-keto-D-glucose, a precursor for the production of vitamins B1 and B6[32,37].

Anaerobic conditions are sometimes extremely important for electroanalytical procedures but they are often difficult to achieve[38]. Therefore, P2Ox can be used as oxygen scavenger to create anaerobic conditions and consequently increase the compound lifetime through the prevention of oxygen-based reactions[39]. With this objective, P2Ox was tested in an oxygen removal system and it was demonstrated that this enzyme is as good as the common scavenging systems but with the advantages of allowing for a long-term pH stability and higher versatility in buffer conditions in terms of ionic strength[39,38].

1.5. Protein engineering

The majority of organisms' native enzymes are not suitable for application in cost-effective industrial bioprocesses due to their poor stability, relatively low reaction rates, product inhibition or limited substrate conversion yields[40]. Protein engineering allows to design enzymes to new or desirable tailor-made properties, appropriate for industrial applications, within short time frames and with the help of a range of strategies that goes from rational computational design to entirely random mutagenic libraries[41]. It is based on the use of recombinant DNA to change protein amino acid sequences[42] and there are three main approaches that can be followed for enzyme engineering: **rational design, semi-rational design** and **directed evolution**.

1.5.1 Methods for introducing mutations in a target gene

The process of **rational design** is the most classical method and deals with preconceived amino acid sequence changes into a target gene through the use of a site-directed mutagenesis (SDM)[42]. This approach is very useful when the structure of a protein is well known, either from a model or a crystal structure, and when it is possible to identify a region of the protein critical for its catalysis or stability[43]. Rational mutagenesis is thus useful to test hypotheses about the structural and functional roles of specific amino acid residues in an enzyme[44]. The 'whole plasmid single round PCR' from Stratagene ('QuickChange SDM kit') is the most commonly approach used to replace specific amino acids into a target gene. In this strategy, two oligonucleotide primers containing the desired mutation(s) to be replaced are constructed (complementary to the opposite strands of a double-stranded DNA plasmid template) and their extension occurs in a PCR reaction through the action of DNA polymerases[44]. Both strands of the template are replicated without the displacement of the primers and a mutated plasmid is obtained with breaks that do not overlap[42]. Afterwards, a selective digestion is performed for the elimination of methylated, non-mutated parent DNA template, and a circular, nicked vector containing the mutant gene is obtained and transformed into competent cells where the nicked vector is repaired by the cell machinery[44]. Finally, mutant proteins are overproduced, purified and characterised, allowing to assess their functional performance[45,46].

The main advantage of **directed evolution**, a 'Darwinian selection' that mimics the natural evolution, is the non-requirement of previous knowledge on structure-function relationships[47]. It relies only on the principle of mutation and selection, and in a first step diversity is created in the parent gene using random mutagenesis or recombination through DNA shuffling, to generate a library of mutant variants[46,48]. In a second step, appropriated methods are used to identify library members that present improved phenotypes through a strategy of selection or screening[49]. The improved variant is used as parent for

the next generation of mutagenesis and screening, and iterative rounds of evolution follow until the desired properties are reached[46] (figure 1.3). Directed evolution has successfully been used to improve characteristics such as substrate specificity, organic solvent resistance, thermostability and up- or down-shifted optimum pH of a large number of enzymes[50]. Random mutagenesis is commonly achieved using *E. coli* mutator strains, chemical mutagenesis or error-prone polymerase chain reaction (epPCR) for the construction of libraries of enzyme variants[47,49]. The most popular method is epPCR which is performed under conditions that conduct to a low fidelity performance of DNA polymerases during DNA synthesis. Usually, a low mutation rate is preferred to ensure a high probability to find beneficial mutations, since most random mutations are either neutral or deleterious[46]. With the aim of controlling the rate of mutation, it is possible to change (1) the number of PCR cycles, (2) the concentration of DNA polymerase, (3) the concentration of $MgCl_2$, (4) the concentration of dNTPs or the use of mutagenic dNTP analogues and, (5) the concentration of $MnCl_2$ in the reaction mixture[51,52]. The drawbacks of this strategy are the high tendency of A → G and T → C nucleotide transitions which lead to a large GC content and the inherent bias introduced by polymerases that limits the type of mutations that can be achieved[46,52]. These inconvenient can be reduced through the use of unbalanced dNTP concentrations and appropriate mixtures of DNA polymerases[49]. The beneficial mutations achieved by this strategy can be subsequently combined through recombination, namely DNA shuffling[53]. Recombination allows the mixture of homologous genes encoding for variants of the same gene or of genes coding for structurally similar proteins of different origin[40,47]. In DNA shuffling, selected genes suffer a controlled fragmentation (~50 to 150 base pairs) with DNaseI and are subsequently combined in an *in vitro* PCR reaction without the need of adding primers since the fragments themselves align and cross-prime to each other[42]. Finally, the small amount of full-length gene present in the reassembly reaction is amplified through the use of appropriate flanking primers in a standard PCR reaction[46]. Among the resulting genes, the most promising ones are selected by screening and isolated[54]. The advantages of this approach is the possibility to accumulate beneficial mutations that can be additive and to eliminate deleterious mutations, which is not possible through the use of non-recombinative strategies as epPCR[55].

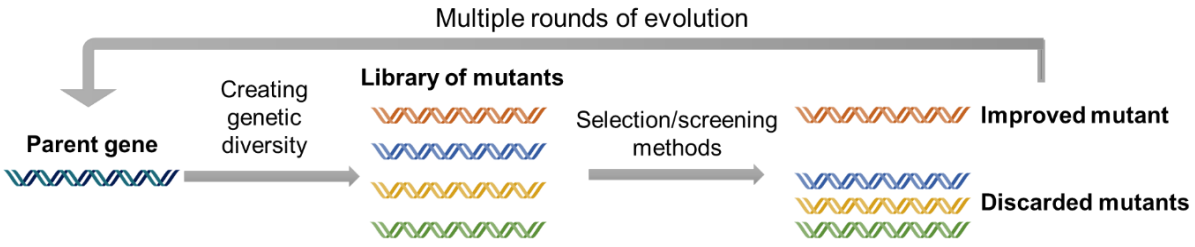

Figure 1.3 Overview of directed evolution of proteins with all steps needed to achieve a desired property: generation of diversity, the choice of a good method of screening/selection, identification of a variant with an improved property and repetition of the cycle until a variant with the desired property is found.

Semi-rational design is a strategy based on the previous knowledge of structure-function relationships *i.e.* of amino acid residues that are important for catalysis, and is useful when a dramatic alteration of the specificity or regioselectivity of the enzyme is required[47]. Through site-saturation mutagenesis

(SSM), it is possible to substitute an amino acid residue for all the other nineteen amino acids available at once. Synthetic oligonucleotides with a randomized codon flanked by wild-type sequences (mutagenic primers) are used to produce every possible amino acid single mutant ('smart libraries')[40]. Due to technical similarities, all methodologies used for SDM can also be applied in SSM with differences in the nature of mutagenic primers; in SSM these are degenerated, *i.e.* a mixture of oligonucleotides that are identical to the parental DNA (allowing the annealing) except for specific targeted positions that permit creating the diversity of amplified products[56]. After a faster and simpler screening, since a smaller library of variants is generated, as compared with random mutagenesis, the best amino acid residue for a given position is chosen considering the property of interest[56,57,58]. There is also the possibility to randomize several codons simultaneously[40].

In addition to above mentioned traditional methods of protein engineering, there is a tool that is becoming increasingly important: computational protein design that is based on the combination of a force field and a search algorithm to identify the amino acid sequence most compatible with a three-dimensional conformation of a given protein[42]. The algorithm has the capability of change at selected positions, the original amino acid to all other nineteen possible amino acids that result in new conformations with different energies[42]. Finally, the conformations that present lower energies are the most favourable and are retained.

1.5.2 Methods of analysis and isolation of variants from a library of mutants

In directed evolution, selection/screening is the most crucial and challenging step and it needs to be sufficiently sensitive and fast enough to find improved variants from large mutant libraries. These can generally be divided in to **selection** and **screening** or *in vivo* versus *in vitro* methodologies. The differences between these strategies are based on how the genotype (genetic information encoding for a protein) and the phenotype (the function of the translated protein) are linked.

In the **selection** strategies there is no need to analyse each library mutant individually due to the presence of a direct link between cell survival or growth and the improved or acquired enzyme function[49]. Selection methods directly eliminate undesired enzyme variants without the requirement of special instruments[49] and their advantages are the possibility of analysing a much larger library of mutants in a reduced time scale[50]. The main disadvantages of the *in vivo* systems relate to the fact that some proteins are toxic for the cells and thus only cellular-harmless enzymes or enzymes that synthetize essential nutrients for cell growth can be engineered, and to the limited genetic diversity that is commonly present due to low transformation efficiencies[40,48].

In **screening** methods, a gene is associated with a certain phenotype (enzymatic activity for a certain substrate, for example) and each mutant protein is evaluated individually for the desired property[50]. The most simple screening is performed in agar plates after growing the library of mutants in the presence of inducer followed by lysis and reaction with enzyme substrates resulting in the formation of a visual sign (fluorescence or colour) that allows for the identification of clones producing improved enzymes[40]. Another common screening method is based in cultivation of the library, disruption and enzyme assays in microtiter plates[40]. Screening methods based on agar or microtiter plates assays only allow to explore a relatively small population of mutants (10^6) which is some orders of magnitude smaller than the library

size[59]. More recently, fluorescence-activated cell sorting (FACS) has appeared as a high sensitivity technique of high-throughput screening that allows to analyse a large number of variants (10^8 per day) of a library, with single cell resolution[60]. In a FACS sorter, cells enter in single droplet form and are illuminated with the use of a focused laser beam. Then, fluorescence of individual cells is measured and a charge is applied to the cells of interest that with the application of an electrostatic field leads to its deflection into a collection tube[59]. The use of fusion reporter proteins provides a very useful tool for single-cell fluorescence analysis and can be used in directed evolution approaches to eliminate inactive variants that present destabilizing mutations[59]. It is possible to couple the activity of a target enzyme to the co-overproduction of a fluorescent protein such as green fluorescent protein (GFP) allowing the set-up of a high-throughput screening of enzyme activities coupled to a FACS system[41]. As the sequence space of proteins is very large, it is almost impossible to explore all mutations that could occur in a protein, which can be considered the major drawback of the directed evolution strategy[43].

1.6 Context of the project

The research focus of the Microbial and Enzyme Technology Lab at ITQB has been to explore enzymes with potential to be used in the areas of health, environmental and industrial biotechnology. The set-up of biocatalytic processes for best performance depends on the development and combination of multidisciplinary research strategies at the biocatalyst level: i) selection of an enzyme with industrial interest, ii) biochemical characterization for providing structural, catalytic and stability fingerprints, iii) engineering to improve their performance and robustness and iv) application to the synthesis, degradation or modification of compounds of interest. The research activities are at the interface of protein science and protein technology, and have focused on the isolation, characterization and engineering of useful bacterial oxidoreductases (laccases, metalloxidases, azoreductases and more recently DyP type peroxidases).

The major aim of this work was to set-up a directed evolution approach to improve the catalytic efficiency of AsP2Ox for D-glucose and dioxygen, with the final purpose of replacing GOx in a large range of industrial and analytic applications. Firstly, we tested the co-production in *E. coli* cells of recombinant AsP2Ox with the Hyper protein (from hydrogen peroxide), a specific fluorescent probe that detect H_2O_2 inside living cells[61], in order to develop a fast and reliable *in vivo* AsP2Ox activity screening method that would allow to discriminate between clones that contain active and inactive AsP2Ox based on the fluorescence of recombinant whole cells[62]. Secondly, several strategies were followed to increase the amounts of soluble AsP2Ox in *E. coli* cells and facilitate the detection of AsP2Ox oxidase activity in cell crude extracts: overproduction of AsP2Ox in various *E.coli* strains, cultivation of cells at different temperatures and culture media, and co-production of AsP2Ox and different chaperones in recombinant cells. Thirdly, the best conditions for mutagenesis and screening of AsP2Ox mutants were identified after optimization and validation of directed evolution protocols at the level of cell growth, lysis and enzymatic assays, in 96 well-plates and in Petri dishes. Finally, a library of 25 000 variants was created by epPCR and screened using a colorimetric high-throughput 'activity-on-plate' assay to detect improved variants of AsP2Ox in the oxidation of D-glucose in the presence of oxygen. A hit 2C9 variant containing 3 mutations was identified and through the complementary use of site-directed mutagenesis

and biochemical characterization of enzyme variants it was possible to unveil the critical role of acquired mutations from the catalytic and structural viewpoints and select the best candidate for a second generation of evolution.

2. Material and Methods

2.1 Bacterial strains, plasmids and media

E. coli strain DH5α (Novagen) was used for routine propagation and amplification of plasmid constructs. *E. coli* Tuner (DE3, Novagen), KRX (Promega) and BL21 star (DE3, Novagen) strains were used to express the genes coding for wild-type AsP2Ox and mutants cloned in pET-15b plasmid (Novagen), the plasmids containing the chaperone genes tested (table 2.1) and the Hyper gene cloned in pET-28b (Novagen). In BL21 star and Tuner strains the target genes are under the control of the T7 promoter, induced by isopropyl β-D-1-thiogalactopyranoside (IPTG), and in the KRX strain the genes are under the control of rhaPBAD promoter, induced by rhamnose. Luria-Bertani medium (LB) and Terrific Broth medium (TB) were used for the maintenance and growth of *E. coli* strains, supplemented with appropriated antibiotics. LB medium contains (per liter): 10 g of tryptone, 5 g of yeast extract and 10 g of NaCl. TB medium contains the following components (per liter): 12 g of tryptone, 24 g of yeast extract, 4 mL of glycerol (86%), 2.3 g of KH_2PO_4 and 12.5 g of K_2HPO_4. Super Optimal Growth medium (SOB) was used for the growth of electrocompetent cells. SOB medium contains (per liter): 20 g of tryptone, 5 g of yeast extract, 0.584 g of NaCl and 0.186 g of KCl. All culture media were sterilized in an autoclave at 121ºC and stored at room temperature until use.

2.2 Preparation of *E. coli* electrocompetent cells

An LB agar plate was streaked out with a frozen stock of *E. coli* cells and incubated overnight at 37ºC. A single colony was picked to inoculate 20 mL of SOB medium and the culture was incubated overnight at 37ºC, 180 rpm. Growth in 500 mL of SOB medium was started at an optical density at 600 nm (OD_{600nm}) of 0.05 and incubated at 37ºC, 180 rpm. After 2.5 h ($OD_{600nm} \simeq 0.8$), cells were transferred to ice-cold centrifuge bottles and spun down (5,000 rpm, 15 min at 4ºC). The supernatant was discarded, and the cell pellets were washed with 250 mL of a sterile ice-cold 10% glycerol solution. The cells were centrifuged, re-washed in 250 mL of the same solution, centrifuged for a third time and re-suspended in 500 µL of the same solution. Aliquots of 150 µL were frozen in liquid nitrogen and stored at -80ºC.

For the co-expression of two recombinant genes in the same *E. coli* strain, first the *E.coli* cells were transformed with the plasmid harbouring the gene encoding for one of the proteins and with the resulting colonies, electrocompetent cells were prepared as previously described. Afterwards, the second plasmid was transformed into these electrocompetent cells so that the co-expression of genes coding for both recombinant proteins is possible.

2.3 Transformation of *E. coli* cells

One microliter of purified plasmids or five microliters of ligation mixtures were added to an aliquot of 150 µL electrocompetent cells (previously thawed on ice) mixed and placed on ice for 5 min. This mixture was transferred to a sterile and ice-cold electroporation cuvette, which was placed in the Xcell ShockPod chamber (Gene Pulser XcellTM, Biorad) and pulsed using set conditions of C = 25 µF, PC = 200 Ω, V = 2.5 kV. Immediately afterwards, 1 mL of LB medium was added; the suspension was transferred to an Eppendorf and incubated at 37ºC for 1 h, 180 rpm. The cells were diluted (to obtain single colonies)

and were spread to an LB agar plate supplemented with appropriate antibiotic and incubated at 37ºC overnight.

2.4 Heterologous expression of target genes

2.4.1 Cell growth of *E. coli* strains overexpressing recombinant genes

2.4.1.1 Overproduction of AsP2Ox at different temperatures

The plasmid pSM-1 (containing the *wild-type asP2Ox* gene) was transformed into *E. coli* BL21 star cells and afterwards the obtained single colonies were used to inoculate 10 mL of LB medium supplemented with 100 µg/mL ampicillin and the cells were grown overnight at 37°C, 180 rpm. Fresh cultures were transferred to two Erlenmeyer flasks containing 20 mL of LB medium supplemented with 100 µg/mL ampicillin, in order to start the growth with an OD_{600nm} = 0.05. Cultures were incubated at 37°C, 180 rpm and when $OD_{600nm} \simeq 0.6$, 100 µM IPTG was added to the cultures and the temperature was decreased to 25°C in one culture and to 10°C in the other culture. In the following day, cells were collected by centrifugation (8,000 rpm, 10 min at 4°C).

2.4.1.2 Co-production of AsP2Ox in the presence of chaperones

From a fresh agar plate, individual E. coli colonies with pSM-1 plasmid and individual colonies presenting both pSM-1 and one of each plasmid present in table 2.1 were picked and transferred to 96-well plates (Sarstedt) containing 200 µL of LB medium supplemented with 100 µg/mL ampicillin (cells containing the pSM-1 plasmid) and with 100 µg/mL ampicillin and 20 µg/mL chloramphenicol (cells containing the additional plasmids). In order to avoid evaporation only the interior wells were used while the peripheral wells were filled with water and plates were sealed with a foil. Cultures were grown for 24 h at 37ºC, 750 rpm in a Titramax 1000 shaker (Heidolph). Twenty microliters were used to inoculate 180 µL of TB medium supplemented with antibiotics in 96-well plates that were incubated at 37ºC, 750 rpm. After 2.5 h of incubation, induction of genes coding for the chaperones (table 2.1) was performed by adding 0.5 mg/mL L-arabinose and/or 5 ng/mL tetracycline, and after more 1 h of incubation, 100 µM IPTG was added to all cultures for the induction of the gene coding for AsP2Ox. The growth proceeded at RT for a 24 h period after which cells were harvested by centrifugation (4,000 rpm, 30 min at 4ºC).

For scaling-up, individual *E. coli* colonies harbouring both pSM-1 and pG-KJE8 plasmids from a fresh agar plate were used to inoculate 20 mL of LB medium supplemented with 100 µg/mL ampicillin and 20 µg/mL chloramphenicol and growth proceeded overnight at 37°C, 180 rpm. Cultures were transferred to two Erlenmeyer flasks containing 100 mL of LB medium supplemented with 100 µg/mL ampicillin and 20 µg/mL chloramphenicol, in order to start growth with an initial OD_{600nm} = 0.05. Cultures were incubated at 37°C, 180 rpm and when $OD_{600nm} \simeq 0.4$, 0.5 mg/mL L-arabinose and 5 ng/mL tetracycline were added and the temperature was decreased to 25°C. When $OD_{600nm} \simeq 0.6$, 100 µM IPTG was added to both cultures. In the next day, cells were collected by centrifugation (8,000 rpm, 10 min at 4°C).

Table 2.1 Plasmid harbouring the *wild-type asP2Ox* gene and plasmids containing genes for the different chaperones that were used in the co-expression using the BL21 star strain.

Plasmids	Proteins	Promotor	Inductor	Resistance	Reference
pSM-1	AsP2Ox	T7	IPTG	Ampicilin	[3]
pGro7	GroES-GroEL	araB	L-Arabinose	Chloramphenicol	Takara Bio Inc
pG-Tf2	GroES-GroEL-Tf	Pzt-1	Tetracycline	Chloramphenicol	Takara Bio Inc
pG-KJE8	DnaK-DnaJ-GrpE GroES-GroEL	araB Pzt-1	L-Arabinose Tetracycline	Chloramphenicol	Takara Bio Inc
pKJE7	DnaK-DnaJ-GrpE	araB	L-Arabinose	Chloramphenicol	Takara Bio Inc
pTf16	Tf	araB	L-Arabinose	Chloramphenicol	Takara Bio Inc
pMJS9	Erv1p-PDI	araB	L-Arabinose	Chloramphenicol	[63]
pFH255	Erv1p-DsbC	araB	L-Arabinose	Chloramphenicol	[63]

2.4.1.3 Co-production of AsP2Ox with Hyper

The plasmid pSM-1 containing the *asP2Ox* gene was transformed into *E.coli* BL21 star, Tuner and KRX strains that were previously transformed with the Hyper-containing plasmid. Single colonies were used to inoculate 10 mL of LB medium supplemented with 100 µg/mL ampicillin (for cells with pSM-1 plasmid only), with 10 µg/mL kanamycin (for cells with Hyper-containing plasmid only) and 100 µg/mL ampicillin plus 10 µg/mL kanamycin (for cells harbouring both the pSM-1 and Hyper-containing plasmids). Cells were grown overnight at 37°C, 180 rpm. These cultures were used to inoculate 20 mL of LB medium supplemented with appropriated antibiotics at a starting OD_{600nm} = 0.05. Cultures were incubated at 37°C, 180 rpm, and when $OD_{600nm} \simeq 0.6$, 100 µM IPTG was added to recombinant *E. coli* BL21 star and Tuner strains, and 0.2 % rhamnose to recombinant *E. coli* KRX and the temperature was decreased to 25°C.

2.4.2 Cell disruption

For cultures grown in 96-well plates, a chemical cell disruption method was employed: cell pellets were suspended in 100 µL of 40% Bacterial Protein Extraction Reagent (B-PER®) lysis solution (Thermo Scientific). After this, plates were centrifuged (4,000 rpm, 30 min at 4ºC) and the supernatant collected (crude extracts).

For cultures grown at larger scales, the cell pellets were suspended in 20 mM Tris-HCl buffer at pH 7.6 containing 5 mM MgCl2, 10 µg/mL DNase I and 5 µg/mL of a mixture of protease inhibitors (antipain and leupeptin). The cell suspensions were disrupted in a French press (Thermo IEC) operating at 900 psi in a process repeated 3 times, allowing for the complete cellular rupture. The lysates were then centrifuged (13,000 rpm, 1 h at 4°C) to separate the non-soluble fraction (i.e. the pellet corresponding to cell debris) from the soluble fraction (crude cell extracts in the supernatant).

2.4.3 Determination of protein concentration

Protein concentration was determined using the Bradford assay with bovine serum albumin (BSA) as standard[64]. A calibration curve was performed with known concentrations of BSA: 0 - 0.6 mg/mL and 20 µL of sample was added to 1 mL or 180 µl (96-well-plate) of Bradford reagent (100 mg of Comassie Blue G dissolved in 45% of ethanol, 100 mL orthophosphoric acid and 750 mL of distilled water, for 1 L of solution), mixed and 10 min later, the absorbance was measured at 595 nm in a spectrophotometer Novaspec III (Amersham Biosciences) or in a Synergy 2 (BioTek) micro plate reader. The protein measurements were performed in triplicate.

2.4.4 SDS-PAGE analysis

Sodium dodecyl sulfate polyacrylamide gel electrophoresis (SDS-PAGE), a method for separating proteins based on the difference of their molecular weight, was utilized to monitor the recombinant protein production as well as the level of protein purification. The running gel was prepared as follows: 12.5% (v/v) acrylamide, "Lower Tris buffer" (375 mM Tris-HCl, 0.1% SDS, pH 8.8), 0.1% (w/v) SDS, 0.1% (w/v) ammonium persulfate (APS), 0.06% (v/v) N, N, N', N'-tetramethylethylenediamine (TEMED). For the stacking gel: 5% (v/v) acrylamide, "Upper Tris buffer" (125 mM Tris-HCl, 0.1% SDS, pH 6.8), 0.1% (w/v) SDS, 0.1% (w/v) APS, 0.1% (v/v) TEMED. The electrophoresis was performed at 220 V during 45 min in the "Electrophoresis Buffer" (192 mM glycine, 25 mM Tris, 0.1% SDS, pH 8.3). Before the application of the protein samples (10 µg of total protein in each well for crude extracts and 1 µg of purified protein) these were mixed with 2 × "Sample Preparation Solution" (2% SDS, 6.255 mM TrisHCl pH 6.8, 5% 2-mercaptoethanol, 0.5 mM DTT, 5% glycerol, and 0.025% bromophenol blue) and denatured at 99°C for 10 min. Gels were stained with Coomassie® blue staining solution (50% ethanol, 10% acetic acid, 0.05% (v/v) Coomassie brilliant blue R-250) with a slow agitation for homogeneous staining. Destaining was performed by using a solution of 10% ethanol and 10% acetic acid.

2.4.5 Enzymatic assays

The activity of AsP2Ox was measured using a horseradish peroxidase (HRP) coupled assay in which the hydrogen peroxide generated by AsP2Ox reaction is used as substrate by the HRP enzyme (Panreac AppliChem) to oxidise two molecules of 2,2'-Azinobis(3-ethylbenzthiazoline-6-sulfonic acid) (ABTS) generating the radical form of ABTS (green) that could be easily monitored at 420 nm (ε = 36,000 M^{-1} cm^{-1})[65]. Reactions were performed at 37ºC in a Nicolet Evolution 300 spectrophotometer from Thermo Industries (Madison). The initial activity in crude cell extracts was measured by adding the enzymatic mixture of 100 mM sodium phosphate buffer at pH 6.5 containing 100 mM of D-glucose, 1 mM ABTS and 10 U HRP. One Unit of P2Ox activity was defined as the amount of enzyme that is necessary for the consumption of 2 µmol of ABTS per min, which equals the consumption of 1 µmol of O_2 per min.

2.5 Fluorescence Microscopy

Cells co-producing heterologous Hyper and AsP2Ox proteins were grown overnight and in the following day 500 µl of each culture was centrifuged (6,000 rpm, 2 min). The cell pellet was suspended in

phosphate-buffered saline (PBS) buffer at pH 7.4 and the cellular suspension was observed in a fluorescence microscope DM6000B (Leica). The images were edited using the MetaMorph® Microscopy Automation & Image Analysis Software. The remaining volume of cell culture was centrifuged (4,000 rpm, 30 min at 4ºC), the pellet was suspended in disruption buffer and disrupted using a French-press as described above and the crude extracts were analysed in terms of protein content by the Bradford method and SDS-PAGE.

2.6 Directed evolution

2.6.1 Random mutagenesis by error-prone PCR (epPCR)

Mutations in the *asP2Ox* gene were generated by using error-prone PCR (epPCR). P2OxFwd (5' CAGGAACTGGTGGCGGGCATATGAGCGGTCACCGGTATCC3') and P2OxRev (5' GCGCTACCGGCTCGAGTTCATTATTTAGACAGTCTATTG 3') flanking the gene beyond the *Nde*I and *Xho*I sites, were used for amplification. The epPCR was carried out in a 50 µL reaction containing 3 ng of DNA template, 1 µM of primers, 200 µM of dNTPs, 1.5 mM $MgCl_2$, Taq polymerase buffer, variable concentrations of $MnCl_2$ (0.01-0.50 mM) to assess the mutation rate, and 2.5 U of Taq polymerase (Thermo Scientific). After an initial denaturation period of 2 min at 95ºC, the following steps were repeated for 30 cycles in a thermal cycler (MyCycler™ thermocycler, Biorad): 1 min at 95ºC, 1 min at 63ºC and 1 min at 72ºC and at the end 10 min at 72ºC. The amplified product (5 µL) was visualized using agarose (1%) electrophoresis in a 40 min-run under an electrical field of 100 V. Afterwards, 10 U of *Dpn*I (Thermo Scientific) were added and the suspension was incubated at 37ºC for 5 h. The final products were purified using the GFX PCR DNA and the Gel Band Purification kit (GE Healthcare) and eluted with mili-Q water. Ten microliters of purified PCR product and 10 µL of pET-15b vector (Novagen) were digested with 10 U of *Nde*I (Thermo Scientific) and 20 U of *Xho*I (Thermo Scientific) at 37ºC for 2 h. The vector pET-15b was simultaneously dephosphorylated with 1 U of alkaline phosphatase (FastAP, Thermo Scientific), to prevent plasmid self-ligation. The products were purified using the GFX PCR DNA and the Gel Band Purification kit (GE Healthcare). The ligations were performed with 0.5 U of T4 DNA ligase (Thermo Scientific) using a 1:3 ratio of vector to insert with 60 ng of vector after a DNA quantification in nanodrop™ 2000c (Thermo scientific). This mixture was incubated overnight at room temperature and then purified using the GFX PCR DNA and the Gel Band Purification kit (GE Healthcare). Transformation into *E.coli* BL21 star was performed as described above.

2.6.2 Overexpression of AsP2Ox and variants in 96-well plates

Individual colonies were picked from a fresh agar plate, and transferred to a 96-well standard plate (Sarstedt) containing 200 µL of LB medium supplemented with 100 µg/mL ampicillin. As previously mentioned, to avoid evaporation only the interior wells were used while peripheral wells were filled with water and the plates were sealed with a foil. Four wells in each plate were used to inoculate the parent of each generation (wild-type was the parent of the first generation). Cultures were grown for 24 h at 37ºC, 750 rpm in a Titramax 1000 shaker (Heidolph). Twenty microliter aliquots were used to inoculate 180 µL of TB medium supplemented with 100 µg/mL ampicillin in 96-well standard plate that was incubated at 37ºC, 750 rpm. After 4 h of incubation, 0.2% rhamnose was added to induce gene

expression in KRX cells and 100 µM IPTG to induce gene expression in BL21 star cells. The growth proceeded at RT for a 24 h period. The cells were harvested by centrifugation (4,000 rpm, 30 min at 4ºC).

2.6.3 Cell disruption in 96 well plates

Four different methods were tested for cell disruption. In the first method, an enzymatic approach was performed where cell pellets in 96-well plates were suspended in 100 µL of 20 mM Tris-HCl buffer at pH 7.6 supplemented with 2 mg/mL of lysozyme. In the second method, cell pellets were submerged in liquid nitrogen and then thawed at room temperature for 5 min. After 3 cycles of freeze and thaw, cell pellets were suspended in 100 µL of 20 mM Tris-HCl buffer at pH 7.6. In the third method, cell pellets were incubated at 80°C for 15 min and then thawed at 37ºC for 5 min. After 3 cycles of freeze and thaw, cell pellets were suspended in 100 µL of 20 mM Tris-HCl buffer at pH 7.6. In the fourth method, a chemical disruption was tested where 100 µL of 40% Bacterial Protein Extraction Reagent (B-PER®) lysis solution (Thermo Scientific) were used to suspend the cell pellets, that were incubated for 15 min at RT with slow agitation. After cell disruption, the suspensions were centrifuged (4,000 rpm, 30 min at 4ºC), the supernatants collected (cell crude extracts) and used for enzymatic activity measurements.

2.6.4 Spectrophotometric high-throughput activity screening using D-glucose and 1,4-BQ as substrates

Fifty microliters of crude cell extracts were transferred to a new 96-well plate and initial activity (Ai) was measured after adding 150 µL of 100 mM sodium phosphate buffer at pH 6.5 containing 10 mM of D-glucose and 1 mM of 1,4-BQ. The absorbance change was followed on a Synergy 2 (BioTek) micro plate reader at 290 nm ($\varepsilon = 2.24\ mM^{-1}cm^{-1}$). The activity of each variant in relation to the parent enzyme was calculated using the ratio of the initial activity of the variant (v) to the parent (p) (A_{iv}/A_{ip}). The variants exhibiting the highest activities were selected and re-screened, to rule out false positives. The selected hit variants from the first generation were grown overnight in 10 mL LB medium supplement with 100 µg/mL ampicillin, at 37ºC, 180 rpm. The plasmid DNA was extracted by using GeneJET Plasmid Miniprep Kit (Thermo Scientific) and mutations identified by DNA sequencing analysis. To identify the codon exchanges and amino acid substitutions, the SnapGene® software was used.

2.6.5 'Activity-on-plate' high-throughput screening using D-glucose and O_2 as substrates

This procedure was based in the lab previous experience in directed evolution "activity-on-plate" screenings[66]. No activity could be detected using *E. coli* KRX cells overproducing pSM-1 (where *asP2Ox*-wild-type was cloned) with this method and consequently all validation was performed using cells of *E. coli* BL21 star transformed with pSM-1 and later with mutant plasmid libraries. After transformation, cells were properly diluted in order to reach a maximum of 200 colonies per plate of solid LB medium supplemented with 100 µg/mL ampicillin and 10 µM IPTG where grown overnight. Colonies were replica-plated onto chromatography paper (Whatman) and the original culture-plate was re-incubated at 37°C until colonies appeared (~ 5 h). The colonies on the filter papers were lysed by carefully soaking the chromatography paper in a solution of 40% Bacterial Protein Extraction Reagent

(B-PER®) lysis solution (Thermo Scientific) because through the enzymatic disruption using lysozyme no activity was observed. The filter papers were then transferred to Petri dishes and dried for approximately 30 minutes at RT. Then the filter papers were soaked in a reaction solution containing 100 mM sodium phosphate buffer at pH 6.5, 10 mM D-glucose, ABTS (1–20 mM) and 10 U HRP, and incubated at RT until a green-purple colour appears (after approximately 2h). The variants showing increased enzymatic activities were identified by the dark purple colour.

2.6.6 Activity re-screening using glucose and O_2 as substrates

All variants showing increased enzymatic activities in the 'activity-on-plate' high-throughput screening were grown in 96-deep well plates (Greiner Bio-One) similar to 96-well standard plates but with 1 mL-volume of culture instead of 0.2 mL-volume and their activity was measured using the HRP coupled assay. The enzymatic assays with 50 µl of crude extracts of variants in a total volume of 200 µl were performed in 100 mM sodium phosphate buffer at pH 6.5 in the presence of 100 mM D-glucose, 10 U HRP and 10 mM ABTS at 37ºC using a Synergy2 microplate reader (BioTek) and rates were calculated based in absorbance differences at 420 nm (ε = 36,000 M^{-1} cm^{-1}). The plasmid DNA of positive clones was extracted by using GeneJET Plasmid Miniprep Kit (Thermo Scientific) and mutations identified by DNA sequencing analysis. To identify the codon exchanges and amino acid substitutions, the SnapGene® software was used. The parent for the next generation was chosen based in the highest initial activity achieved among the various variants.

2.7 Site-directed mutagenesis

Single and double amino acid substitutions in the asP2Ox gene were created using the Quick Change mutagenesis protocol (Stratagene). The plasmid pSM-1 (containing the asP2Ox-wild-type gene) was used as DNA template with appropriated primers (table 2.2) and the plasmid obtained after the insertion of the F300V mutation was used as template to insert A35T mutation to produce the double mutant. PCRs were performed in a thermal cycler (MyCyclerTM Thermal Cycler, Biorad) in 50 µL reaction volumes containing 3 ng of DNA template, 1 µM of primers, 200 µM of dNTPs (NZYTech), NZYProof polymerase buffer, and 1.3 U of NZYProof polymerase (NZYTech). The conditions used for performing the PCR reactions are listed in table 2.3. The amplified product was digested with 10 U of DpnI (Thermo Scientific) at 37ºC for 5 h to eliminate the wild-type template and visualized through an agarose (1%) gel in a 40 min-run under an electrical field of 100 V. The resulting product was purified using GFX PCR DNA and Gel Band Purification kit (GE Healthcare) and used to transform electrocompetent E. coli DH5-α cells. The presence of the desired mutation(s) in the resulting plasmid and the absence of additional mutations in other regions of the insert were confirmed by DNA sequencing.

Table 2.2 Primers used in the site-directed mutagenesis for the construction of different mutants. Fwd-primer forward; Rev-primer reverse. The nucleotides in bold and underlined correspond to the base substitutions.

Mutation		Primer
A35T	Fwd	5'-GGAAGCCCCCGGT**A**CCACGATCGCGATGTTCGAAGTGG-3'
	Rev	5'-CCACTTCGAACATCGCGATCGTGG**T**ACCGGGGGCTTCC-3'
F300V	Fwd	5'-CCTGAACGACCAGGCGCAGGTG**G**TGGTCGCGAGCAGGC-3'
	Rev	5'-GCCTGCTCGCGA**C**CACCACCTGCGCCTGGTCGTTCAGG-3'

Table 2.3 Conditions used in the PCR reactions for the construction of different mutant enzymes using site-directed mutagenesis.

Mutant	Denaturation	Cycles	Number of cycles	Final amplification
A35T	4 min at 95ºC	95°C : 1 min 70°C: 1.5 min 72°C: 10 min	22	10 min at 72°C
F300V	4 min at 95ºC	95°C : 1 min 72°C: 1.5 min 72°C: 10 min	25	10 min at 72°C
A35T/F300V	4 min at 95ºC	95°C : 1 min 70°C: 1.5 min 72°C: 10 min	22	10 min at 72°C

2.8 Production and purification of wild-type and recombinant AsP2Ox variants

For the production of wild-type AsP2Ox and variants at a larger scale, single colonies were used to inoculate 50 mL of LB medium supplemented with 100 µg/mL ampicillin, which were grown overnight at 37ºC, 180 rpm. These cultures were used to inoculate 1 L of LB medium in 5L-Erlenmeyer flasks, supplemented with 100 µg/mL ampicillin, in order to start the growth with an OD_{600nm} = 0.05. Cultures were incubated at 37ºC at 180 rpm and when $OD_{600nm} \simeq 0.6$, 100 µM IPTG was added. After 24 h of cultivation, cells were collected by centrifugation (8,000 rpm, 15 min at 4ºC) and the cellular pellets were re-suspended in the same conditions mentioned above and were disrupted in a French press (Thermo IEC) operating at 1000 psi in a process repeated 5 times, allowing for the complete cellular rupture. Cell debris was removed by centrifugation (18,000 rpm, 2h at 4ºC) and crude extracts were filtrated with a 0.2 µm membrane to remove large particles in suspension prior to loading onto the chromatographic column. The protein purification was performed in an ÄKTA purifier (GE Healthcare). The crude extract was loaded onto a 1 mL HisTrap HP column (GE Healthcare) equilibrated with 20 mM Tris-HCl buffer at pH 7.6 supplemented with 0.2 M NaCl and 10 mM imidazole. Elution was carried with a 0-100% gradient of imidazole (1 M) with a flow rate of 1 mL/min. The yellow fractions were collected, desalted using a PD-10 desalting column (GE Healthcare), concentrated in 20 mM Tris-HCl buffer at pH 7.6 with 0.2 M NaCl and stored in buffer with 20% of glycerol at −20ºC.

2.9 Spectroscopic analysis of FAD-ligation

UV–Visible absorption spectra of the purified enzyme were recorded at room temperature by using a Nicolet Evolution 300 spectrophotometer from Thermo Industries (Waltham). For identification of the flavin cofactor, a preparation of purified AsP2Ox was treated with 0.4% (w/v) of SDS and the UV–Vis spectrum was recorded[67]. Alternatively, 5% trichloroacetic acid was added to a purified protein preparation and heated at 100ºC for 10 min. After centrifugation (13,000 rpm, 10 min) a UV-Vis spectrum was recorded.

2.10 Kinetic analysis

The enzymatic activity of purified wild-type AsP2Ox and mutants proteins was monitored using a Nicolet Evolution 300 spectrophotometer (Thermo Industries) and a Synergy2 microplate reader (BioTek) where the formation of product was monitored at 420 nm (ε = 36,000 M^{-1} $cm^{-1)}$. All enzymatic assays were performed at least in triplicate. The routine reaction mixture contained 1 mM ABTS, 10 U HRP, 1 M D-glucose and was saturated with pure oxygen prior to initiation with enzyme. One unit of AsP2Ox activity was defined as the amount of enzyme necessary for the oxidation of 2 µmol of ABTS (equivalent to the oxidation of 1 µmol of D-glucose) per min under the assay conditions.

All steady-state kinetic measurements were performed at 37ºC in 100 mM sodium phosphate buffer at pH 6.5. Apparent steady-state kinetic parameters (k_{cat} and K_m) were measured for D-glucose in oxygen-saturated solutions using the routine ABTS-peroxidase assay. Kinetic data were fit directly into the Michaelis-Menten equation (Origin-Lab software).

3. Results and Discussion

3.1 Development of an *in vivo* activity screening for AsP2Ox

In order to develop an activity screening that would avoid time consuming cell disruption procedures and enzymatic activity assays, the co-production of AsP2Ox and Hyper protein, a specific fluorescent probe that detect H_2O_2 inside living cells was tested (figure 3.1). This probe consists of a circularly permuted yellow fluorescent protein (cpYFP) inserted into the regulatory domain of a prokaryotic H_2O_2-sensing protein (OxyR) which demonstrates submicromolar affinity to H_2O_2 and insensitivity to other oxidants[61]. The Hyper protein has a cysteine residue that reacts with H_2O_2, leading to the formation of a disulfide bond, that results in a conformational alteration, and subsequent change in the excitation spectrum[62]. The fluorescent signals of Hyper show two excitation peaks at 420 and 500 nm that upon exposure to hydrogen peroxide result in a proportional decrease of the excitation band at 420 nm and an increase of the band at 500 nm[61]. The utilization of this system based on the fluorescent properties of Hyper would allow to easily eliminating inactive mutants in a library of variants[62].

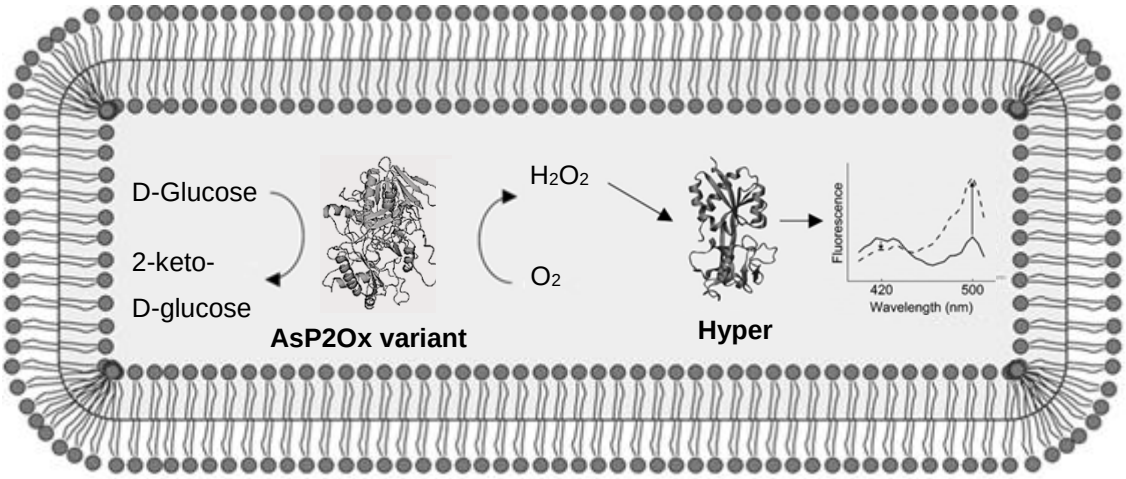

Figure 3.1 Hyper-based screening for *in vivo* detection of enzymatic H_2O_2 production. The objective was to identify better variants of AsP2Ox through a higher production of H_2O_2 that would result in an increased excitation spectrum of Hyper at 500 nm and a decrease at 420 nm. The reduced spectrum is shown as a solid line and the oxidized spectrum as a dashed line. Adapted from[62].

With this objective, AsP2Ox and Hyper were co-produced in BL21 star cells, the strain previously known to result in the highest production of both proteins. Different cells were grown: cells producing only AsP2Ox, cells producing only the Hyper protein and cells co-producing both AsP2Ox and Hyper proteins. After cultivation, cells were visualized using a fluorescence microscope (figure 3.2). As expected, no fluorescence was present in cells where only AsP2Ox is produced. In cells producing only the Hyper protein, it was possible to observe a drastic change in the fluorescence and also in the shape and dimensions of cells: they become much larger when compared with cells only producing AsP2Ox and intracellular inclusion bodies are visible. The higher fluorescence intensity observed is most probably due to H_2O_2 present in the cytoplasm of cells, originated from the cellular oxidative stress, that is also visible in non-induced cells probably due to a leakage in the expression of the Hyper gene in the

absence of inducer. Even though cells that produce both AsP2Ox and Hyper proteins showed a slight higher dimension and fluorescence, there are no sufficient differences as compared with cells that only produce the Hyper protein that could allow the implementation of a FACS-based screening system (figure 3.2). The cell crude extracts of the above mentioned cultures were analysed by SDS-PAGE (figure 3.3) where it is possible to observe that both proteins were overproduced in induced cultures.

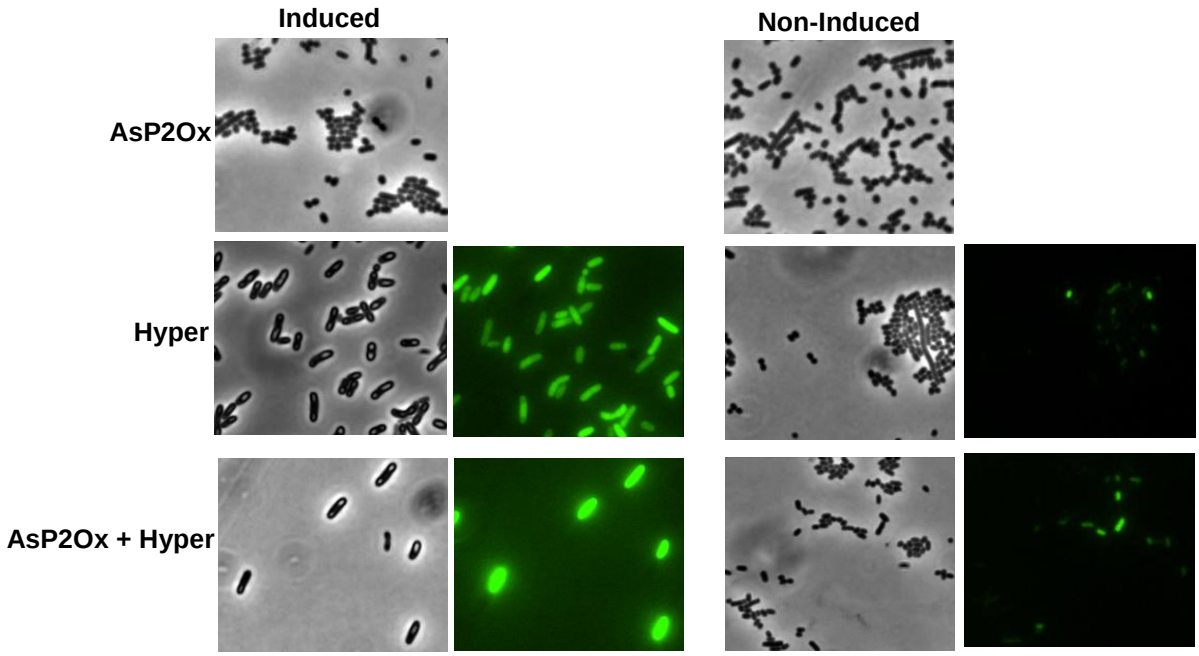

Figure 3.2 Images of induced and non-induced cell cultures obtained by bright-field and fluorescence microscopy producing AsP2Ox, Hyper and co-producing both proteins in the BL21 star strain. When only AsP2Ox was produced, no fluorescence was detected as expected.

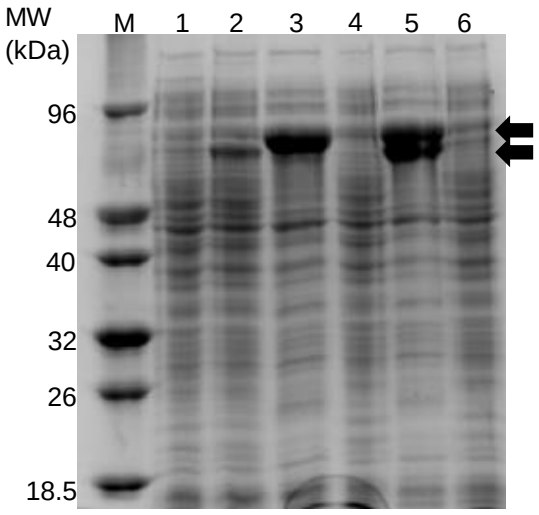

Figure 3.3 SDS-PAGE of BL21 star crude extracts. (M) Marker, non-induced (1) and induced (2) cell extracts overproducing AsP2Ox, induced (3) and non-induced (4) cell extracts overproducing Hyper and, induced (5) and non-induced (6) cell extracts overproducing both AsP2Ox and Hyper proteins. The arrows show the bands that correspond to the AsP2Ox protein (~64 kDa) and to the Hyper protein (~66 kDa).

In an attempt to find a strain that allows better differentiate the fluorescence intensity between cells producing only Hyper and cells co-producing both Hyper and AsP2Ox proteins, two additional recombinant *E.coli* strains were tested: KRX and Tuner strains (figure 3.4). No fluorescence was detected in Tuner cells, indicating that the Hyper protein is not produced by this strain. With KRX cells, a low fluorescence intensity was detected with no major differences when only Hyper or both AsP2Ox and Hyper proteins were produced, even though the dimensions, shape and fluorescence of cells were not so dramatically changed as observed when BL21 star cells were used. These results were confirmed by the SDS-PAGE analysis where the protein bands that correspond to AsP2Ox and Hyper proteins were barely observed (figure 3.5).

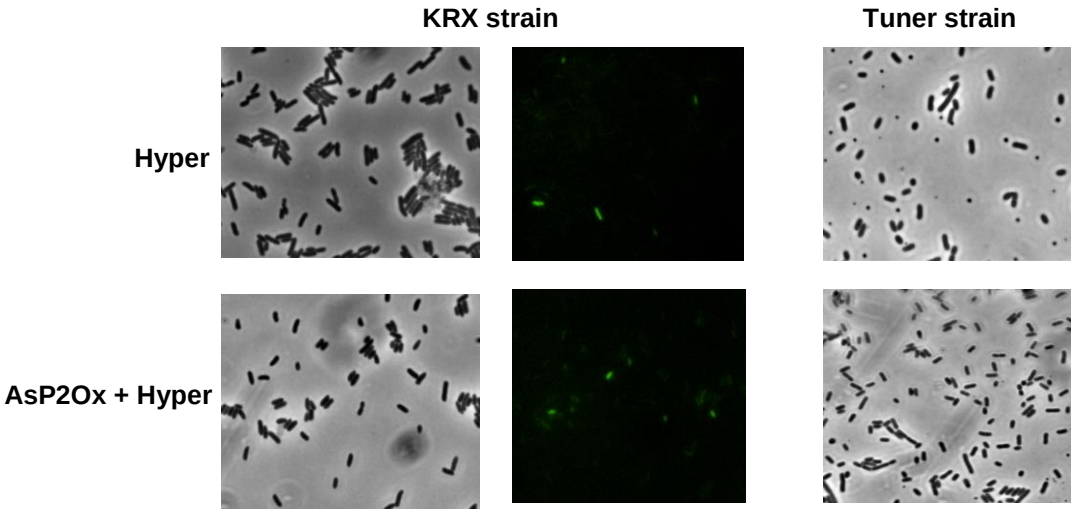

Figure 3.4 Images of cell cultures obtained by bright-field and fluorescence microscopy producing Hyper and co-producing both proteins (AsP2Ox and Hyper) in KRX and Tuner strains. No fluorescence was detected when Tuner strain was used as expression strain.

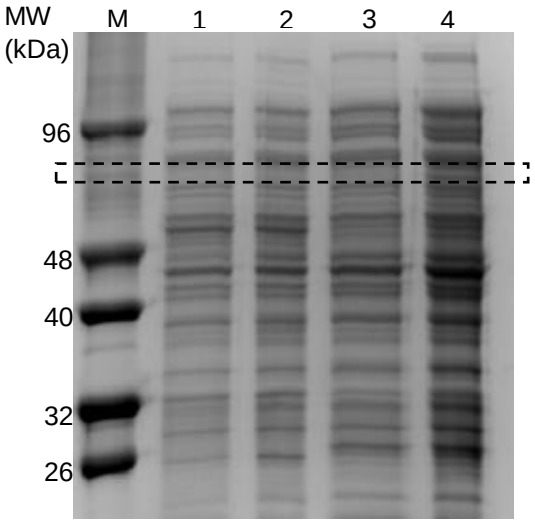

Figure 3.5 SDS-PAGE of KRX and Tuner crude extracts. (M)-Marker, (1) KRX cell extracts overproducing Hyper, (2) KRX cell extracts overproducing Hyper and AsP2Ox, (3) Tuner cell extracts overproducing Hyper and (4) Tuner cell extracts overproducing AsP2Ox and Hyper. AsP2Ox has a molecular weight of 64 kDa and Hyper of 66 kDa approximately.

In conclusion, the Tuner strain is not suitable for the production of both proteins due to the lack of expression of the correspondent genes. On the other hand, the use of BL21 star or KRX cells for the co-production of both Hyper and AsP2Ox proteins is not suitable for a FACS-based activity screening of AsP2Ox due to the high "auto"-fluorescence of Hyper in the absence of AsP2Ox enzyme production. These results showed that there is a high amount of H_2O_2 inside the cells, possibly resulting from cellular oxidative stress that can oxidise the Hyper protein, thus preventing the identification of improved AsP2Ox variants.

3.2. Optimization of growth conditions to increase the solubility of recombinant AsP2Ox in *E. coli* cells

A large amount of recombinant AsP2Ox overproduced in *E. coli* cells is present in the insoluble fraction, most likely in the form of inclusion bodies (figure 3.6). Inclusion bodies result from the intracellular accumulation of partially folded produced proteins that aggregate through hydrophobic or ionic interactions or a combination of both in the cytoplasm of *E. coli* [14]. The relatively low amounts of soluble AsP2Ox enzyme in crude extracts of *E. coli*, associated with the very low detected specific activity of purified enzyme for molecular oxygen (k_{cat}/K_m = 0.03 $M^{-1}s^{-1}$) resulted in the absence of detected activity for AsP2Ox using O_2 as electron acceptor in crude cell extracts of *E. coli*. This fact prevents the development of an appropriate activity screening strategy using as substrates D-glucose and O_2 in the process of directed evolution.

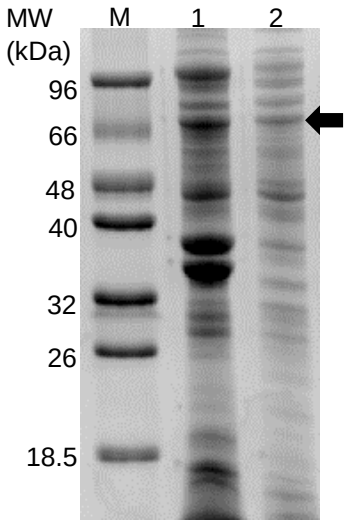

Figure 3.6 SDS-PAGE performed with the insoluble and soluble fractions of recombinant *E. coli* cell extracts of cells overproducing AsP2Ox. (M) marker, (1) insoluble fraction and (2) soluble fraction. The arrow shows the band that corresponds to the AsP2Ox protein (~64 kDa).

With the aim of increasing the soluble production of AsP2Ox enzyme, the temperature of the growth cultures was reduced from 37 to 25 and 10ºC after induction with IPTG. A decrease in temperature is expected to result in a decrease of bacterial growth rate and in an increase of soluble protein content[14]. It was possible to visualize in the SDS-PAGE (figure 3.7) that a higher amount of AsP2Ox protein was achieved in the soluble fraction upon incubation at 25ºC after IPTG induction as compared with 10ºC.

In spite of the absence of activity using O_2 as electron acceptor in both crude extracts, in further studies, the temperature of growth was shifted from 37 to 25ºC after IPTG induction.

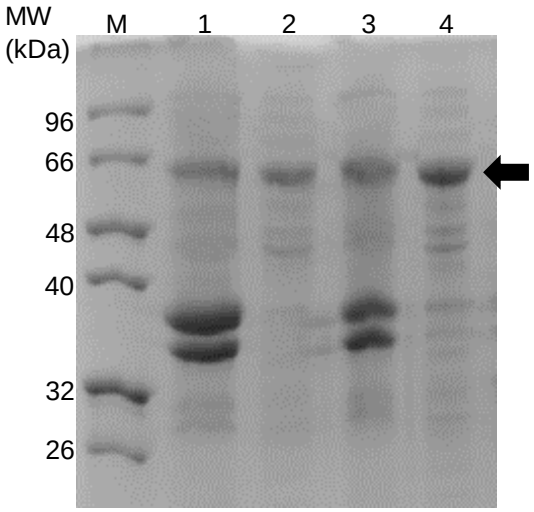

Figure 3.7 SDS-PAGE of insoluble and soluble fractions of cells grown at different temperatures after IPTG induction. (M) marker, insoluble (1) and soluble fraction (2) of crude extracts of cells incubated at 10ºC after IPTG induction and insoluble (3) and soluble fractions (4) of crude extracts of cells incubated at 25ºC after IPTG induction. The arrow indicates the band that corresponds to AsP2Ox (~64 kDa).

As an alternative strategy for the prevention of inclusion body formation, the co-production of AsP2Ox protein in the presence of recombinant molecular chaperones was performed. In our laboratory there are seven plasmids encoding for different chaperones (table 3.1) and all were co-produced with AsP2Ox in *E. coli* cells cultivated in 96-well plates. As observed in Table 3.1, very high coefficients of variation (CV = standard deviation/mean x 100 %) both in the values of the final OD_{600nm} of cultures and protein concentration in crude extracts were observed. Importantly, when activity was tested using D-glucose and O_2 as electron acceptor, only the reaction mixtures using crude extracts of cells co-producing AsP2Ox and DnaK-DnaJ-GrpE-GroES-GroEL chaperones (pG-KJE8 plasmid) showed a very tenuous green colour, characteristic of the cation radical $ABTS^{\bullet+}$ formation, and indicative of enzyme reaction activity. Based in this result a larger scale (100 mL) culture using this co-production system was performed.

Table 3.1 Final OD_{600nm} of cell cultures co-producing AsP2Ox and different chaperones and protein concentration in cell crude extracts.

Plasmids	Chaperones	Molecular weight (kDa)	OD_{600nm}	CV (%)	Protein (mg/mL)	CV (%)
pGro7	GroES-GroEL	10; 60	0.7 ± 0.5	71	0.4 ± 0.2	50
pG-Tf2	GroES-GroEL-Tf	10; 60; 56	0.5 ± 0.4	80	0.2 ± 0.2	100
pG-KJE8	DnaK-DnaJ-GrpE GroES-GroEL	70; 40; 22; 10; 60	0.3 ± 0.2	67	0.2 ± 0.2	100
pKJE7	DnaK-DnaJ-GrpE	70; 40; 22	0.3 ± 0.3	100	0.2 ± 0.2	100
pTf16	Tf	56	0.6 ± 0.4	67	0.4 ± 0.2	50
pMJS9	Erv1p-PDI	32; 56.7	0.6 ± 0.4	67	0.3 ± 0.1	33
pFH255	Erv1p-DsbC	32; 47.2	0.5 ± 0.4	80	0.3 ± 0.2	67

Two cultures co-producing AsP2Ox and selected chaperones (pG-KJE8 plasmid) were performed: one where the chaperones were induced and a second where the chaperones were not induced. In the SDS-PAGE the production of chaperones with 22, 40, 60 and 70 kDa is visible in fractions of crude extracts of induced as compared with those from non-induced cells (figure 3.8).

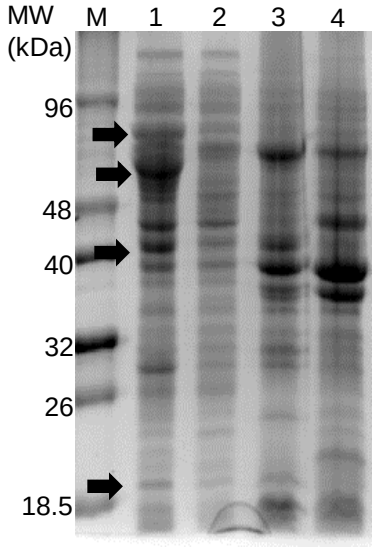

Figure 3.8 SDS-PAGE of insoluble and soluble fractions of induced and non-induced cells overproducing AsP2Ox and chaperones. (M) marker, soluble fractions of crude extracts where genes coding for chaperones were induced (1) and non-induced (2), insoluble fractions of crude extracts of cells where genes coding for chaperones were induced (3) and non-induced (4). Black arrows correspond to chaperone proteins: GrpE, DnaJ, GroEL and DnaK that present molecular weights of 22, 40, 60 and 70 kDa respectively.

The above mentioned results are supported by the 6-fold higher protein concentration in crude extracts of induced (5.8 ± 0.5 mg/mL) as compared with non-induced cells (1.0 ± 0.1 mg/mL). It was not possible to assess in the SDS-PAGE (figure 3.8) the putative increased production of AsP2Ox in soluble fractions

of crude extracts of cells where the chaperones were induced due to the fact that both GroEL and DnaK chaperones have a molecular weight (60 ; 70 kDa) very close to AsP2Ox (64 kDa). However, when enzymatic activity was tested in crude extracts, no improvement was detected indicating that the presence of chaperones apparently did not result in an increased production of soluble AsP2Ox as desired.

3.3 Directed Evolution of AsP2Ox

3.3.1 Validation of high-throughput screenings in 96-well plates

As previously mentioned, the most crucial step of directed evolution is to set-up procedures that allow identifying the desired mutants minimizing the selection of false positives. For this, several experiments need to be performed in order to develop, validate and implement methods at the level of cell growth, protein production, cell lysis and activity screening assays in 96-well plates[68].

3.3.2 Selection of the best conditions to overexpress *asP2Ox* in *E.coli*

The *E. coli* strain that leads to a higher production of AsP2Ox was previously known to be the BL21 star. In this work the capabilities of the *E. coli* KRX strain for the overproduction of AsP2Ox were tested since this strain acts as a cloning as well as an expression strain, which would avoid additional steps of plasmid transfer among strains in the evolution process. With this aim, both strains BL21 star and KRX were grown in 96-well microplates in two different growth media: LB and TB, in order to choose the conditions that result in minimal variations in the growth and production of the enzyme of interest. After cell lysis with B-PER® solution and centrifugation, protein concentration and specific activity using 1,4-BQ as electron acceptor was monitored in crude extracts. The substrate used was 1,4-BQ because with O_2 no activity can be observed in crude extracts (table 3.2).

Table 3.2 Final OD_{600nm} of cell cultures of BL21 star and KRX strains grown in different media, protein concentration and specific activity in crude cell extracts. Enzymatic assays were performed at 37ºC, in 100 mM sodium phosphate buffer at pH 6.5 in the presence of 10 mM D-glucose and 1 mM 1,4-benzoquinone.

Strain		OD_{600nm}	CV (%)	[Protein] (mg/mL)	CV (%)	Specific Activity (nmol/min.mg)	CV (%)
BL21 star	LB	1.0 ± 0.3	30	0.4 ± 0.1	25	24 ± 9	38
	TB	1.2 ± 0.4	33	0.6 ± 0.2	33	22 ± 8	36
KRX	LB	0.7 ± 0.3	43	0.3 ± 0.1	33	102 ± 127	125
	TB	1.2 ± 0.6	50	0.5 ± 0.3	60	86 ± 106	123

The obtained results show that lower coefficients of variation were achieved with BL21 star as compared to the KRX strain in all steps of the screening process. Moreover, no major CV differences were observed in protein content and enzyme activities in crude extracts of BL21 star cells grown in LB or TB media. Therefore BL21 star grown in TB medium was chosen for further experiments since a higher concentration of protein is present in crude extracts, a lower CV was obtained for specific activity and a

stronger yellow colour (characteristic of flavin proteins) was visible in crude extracts, an indication of higher amounts of AsP2Ox in solution.

3.3.3 Selection of the cell disruption method in 96-well plates

After selecting the *E.coli* strain and cultivation medium for the screening process the most appropriate cell disruption method was identified. Four methods of cell disruption were tested (table 3.3). The first was an enzymatic method that uses lysozyme, an enzyme that catalyzes the hydrolysis of β (1→4) linkages between the N-acetylmuraminic acid and the N-acetyl-D-glucosamine residues in the peptidoglycan of bacterial cell walls. The utilization of this method resulted in a high coefficient of variation in the specific activity.

The low-temperature physical methods putatively result in the formation of small pores in the bacterial membrane/wall that allow soluble overproduced proteins to be released without causing total destruction of the cells[69]. In the first method tested, cells were submitted to three cycles of freezing with liquid nitrogen following by thawing at room temperature and, in the second method tested, cells were subjected to three cycles of freezing at - 80ºC for 15 min and then thawing at 37ºC for 5 minutes. By following these methods, the concentration of total protein was ~6 times lower and the specific activity 5-fold higher when compared to the enzymatic method (table 3.3). This result may indicate that the passage of intracellular proteins through the pores of cellular walls to the outer space somehow benefit the passage of AsP2Ox. However, the coefficients of variation using both physical methods were considered too high for an accurate screening of variant libraries.

Finally, a fast chemical method was tested, the commercial B-PER® solution containing a non-ionic detergent. The application of this solution resulted in a concentration of protein 2-fold lower and 3-fold higher compared to those achieved with the enzymatic and the physical methods, respectively, while the specific activities are similar and ~3 times lower to that observed with enzymatic and the physical methods, respectively (table 3.3). However, the lowest coefficients of variation both in terms of protein concentration and specific activity were achieved, putatively leading to a lower probability of finding false positive clones during the evolution process of AsP2Ox, and this method was therefore chosen for further experiments.

Table 3.3 Protein concentration and specific activity in crude extracts after using different disruption methods. Cells were disrupted using enzymatic (lysozyme 2 mg/mL), physical (freeze/thaw using Liquid Nitrogen (LN)) or freeze/thaw through incubation at -80ºC) and chemical (B-PER® lysis solution) methods.

Disruption Method		[Protein] (mg/mL)	CV (%)	Specific Activity (nmol/min.mg)	CV (%)
Enzymatic	Lysozyme 2 mg/mL	1.1 ± 0.4	36	13 ± 12	92
Physical	Freeze/Thaw (LN_2)	0.2 ± 0.1	50	64 ± 46	72
	Freeze/Thaw (-80ºC)	0.2 ± 0.1	50	44 ± 25	56
Chemical	B-PER	0.6 ± 0.2	33	22 ± 8	36

3.3.4 Generation of AsP2Ox mutant libraries using epPCR

In general, the finest strategy in directed evolution is to obtain libraries of mutants that present a low number of mutations because this eliminates the possible accumulation of neutral or deleterious mutations, since increased mutation rates are proportional to a decreased number of functional protein variants[51]. In general, a mutation rate of ~1-3 nucleotides per gene correspond to a library with 30-40% of mutants having less than 10% of the parent enzyme's activity ('dead' mutants) and this is considered the appropriate rate for directed evolution strategies[51].

The variation of manganese chloride ($MnCl_2$) concentration in the PCR reaction, is one of the parameters that allows to adjust the mutation rate in the gene of interest[51]. With this objective, six libraries were constructed with increasing concentrations of $MnCl_2$ (0.01-0.5 mM) to test which concentration led to the desired mutation rate of ~1-3 nucleotides in the *asP2Ox* gene. The enzymatic activities of 54 clones of each library were tested in 96 well-plates (1 plate per library) and compared to the wild-type AsP2Ox (figure 3.9). As expected, the number of "dead" mutants increased with the manganese chloride concentration in the PCR reaction. In the presence of 0.01 mM and 0.10 mM $MnCl_2$ all clones showed an activity higher than 10% of the parent enzyme's activity while using 0.20, 0.30, 0.40 and 0.50 mM $MnCl_2$, 2%, 9%, 13% and 37% of inactive clones were observed, respectively.

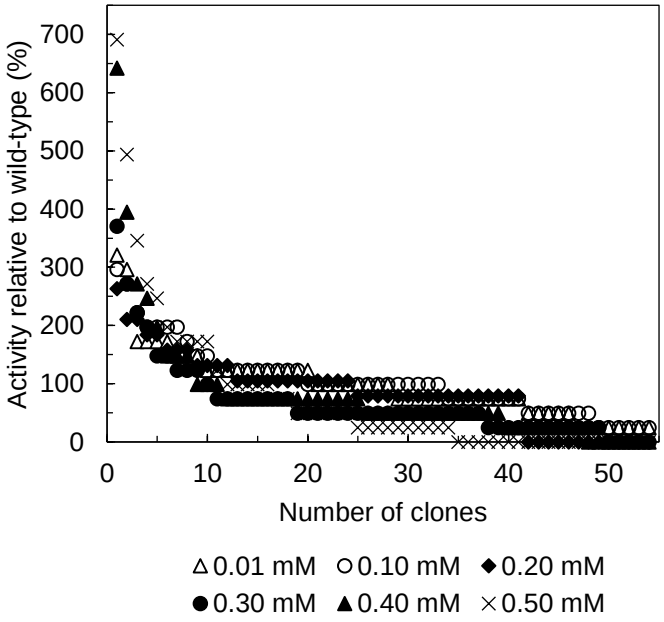

Figure 3.9 Landscape correspondent to six variant libraries using different $MnCl_2$ concentrations: 0.01 mM (△), 0.10 mM (○), 0.20 mM (♦), 0.30 mM (●), 0.40 mM (▲) and 0.50 mM (x). Activity of clones relative to the wild-type is plotted in descending order.

Based on these results, the concentration of $MnCl_2$ chosen for random mutagenesis in the directed evolution procedure of AsP2Ox enzyme was 0.5 mM because it would hypothetically allow to obtain the desired rate of mutation corresponding to ~1-3 base substitutions[51] in the *asP2Ox* gene.

3.3.5 High-throughput activity screening of the mutant library using 1,4-BQ as electron acceptor

The catalytic efficiency of purified AsP2Ox for D-glucose using oxygen as electron acceptor is 4 orders of magnitude lower when compared with 1,4-BQ. Consequently, no activity using oxygen as electron acceptor was detected in crude cells extracts growing in standard 96-well plates in any condition tested (table 3.2 and 3.3). For this reason, it was decided to screen the first generation of evolution using 1,4-BQ as substrate.

A total of 2 052 clones were screened (figure 3.10-A). Owing to the relative high coefficient of variation in the specific activity measured for the wild-type enzyme (36%), all clones that presented an activity 2.5 times higher as compared with the wild-type parent (66 clones) were re-screened in order to decrease the number of false positives (figure 3.10-B). After the re-screening, three clones 19C11, 26C11 and 14B3 that have shown specific activities 4, 3 and 3 times higher than the parent, respectively, were selected, plasmids were extracted, transformed on DH5-α cloning strain, purified and sent to sequencing.

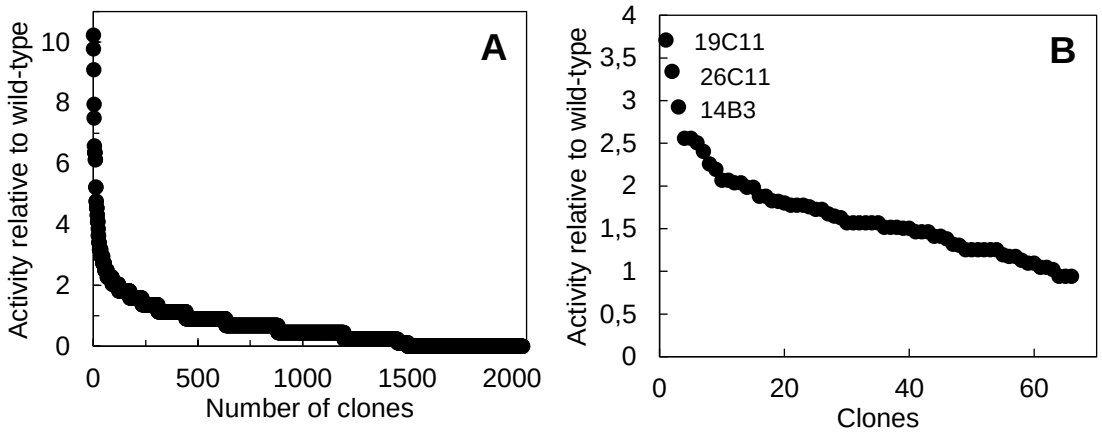

Figure 3.10 Directed evolution landscape corresponding to the first generation of mutants. (A) Activity relative to wild-type of 2052 clones screened in the first generation. (B) Re-screening of the best 66 variants found in the first generation. Enzymatic assays were performed at 37ºC, in 100 mM sodium phosphate buffer at pH 6.5 in the presence of 10 mM D-glucose and 1 mM 1,4-benzoquinone.

The sequencing results have unfortunately shown that genes from the variants were wild-type *asP2Ox*, representing false positive clones. New epPCR were performed followed by digestion with *Dpn*I to eliminate wild-type plasmid, and DNA from five random clones from each library was purified and sequenced. The results showed that using 0.5 mM $MnCl_2$ in the PCR reaction, resulted in 12 substitutions per gene, and that the concentration of $MnCl_2$ that produced the desired rate of 1-3 base substitutions per gene was around 0.01 mM (table 3.4). These results were surprising considering the previous experience in the laboratory and the data in the literature. However, it was decided to generate a new library of mutants by epPCR in the presence of 0.01 mM $MnCl_2$.

Table 3.4 Average of base substitutions in the *asP2Ox* gene after epPCR performed in the presence of different concentrations of manganese chloride. Four to five clones were randomly selected from libraries generated after epPCR at different $MnCl_2$ concentrations, plasmids were extracted, transformed on DH5-α cloning strain, purified and sent to sequencing.

[$MnCl_2$] (mM)	**Base substitutions average**
0.01	1
0.10	1
0.20	6
0.30	16
0.40	9
0.50	12

3.3.4. "Activity-on-plate" high-throughput activity screening using O_2 as electron acceptor

To test the new library of variants it was decided to try a different strategy: an 'activity-on-plate' screening, a colorimetric assay developed and validated using BL21 star overproducing wild-type AsP2Ox. This qualitative strategy allows for the screening of a higher number of variants in a shorter period of time when compared to the 96-well plate activity screening since it eliminates the step of picking individual colonies from agar plates and growing cells in liquid medium. Moreover and importantly, it allows identifying variants of AsP2Ox with higher oxidative activity since the lysed colonies are tested for the oxidation of D-glucose in the presence of oxygen by following a coupled assay with HRP in the presence of ABTS. The differences observed in the colour of lysed colonies are the result of the ABTS oxidation. For this screening, colonies present on the solid media, resultant from growth of BL21 star cells transformed with the mutant library in the presence of IPTG, were transferred to a Whatman chromatography paper and soaked in a solution of B-PER® 40%. Next, the paper containing the lysed colonies is soaked in enzymatic reaction mixture containing D-glucose, HRP and ABTS and improved variants are identified through the darker colour presented (figure 3.11).

Figure 3.11 Overview of 'activity-on-plate' screening used for the directed evolution of AsP2Ox enzyme.

When the colonies were grown on agar medium in the absence of inducer (IPTG), as expected, no activity was observed (figure 3.12-A). Immediately after soaking the disrupted cells grown in the presence of IPTG in the reaction mixture with 20 mM ABTS (figure 3.12-B), a strong green colour appeared that quickly changed to a dark purple. These two colours are due to the existence of two relatively stable and electrochemically reversible oxidation states of ABTS: the cation radical $ABTS^{\bullet+}$ (green) and the dication $ABTS^{2+}$ (dark purple)[70]. Considering that at the conditions tested an intense purple colour was observed, the concentration of ABTS was decreased from 20 to 1 mM (figure 3.12-C-E) and with this later concentration, it was seen just a weak purple colour that appeared 2 hours after the filters had been soaked in the reactional mixture.

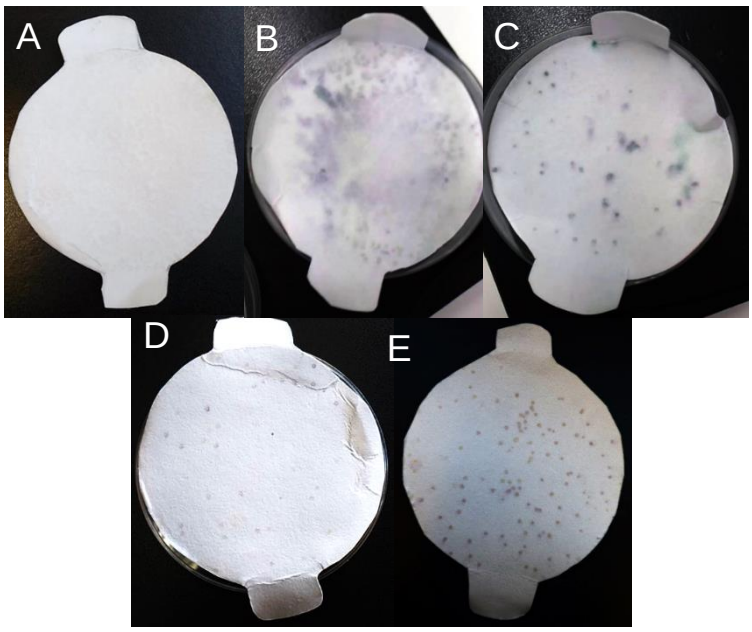

Figure 3.12 'Activity-on-plate' high-throughput assay (with 10 U HRP and 10 mM D-glucose) using BL21 star cells transformed with wild-type AsP2Ox plasmid and grown in LA media in the presence of 10 μM IPTG. (A) Non-induced cells incubated in the presence of 20 mM ABTS. Cells overexpressing *asP2Ox* gene in the presence of (B) 20 mM, (C) 10 mM, (D) 5 mM and (E) 1 mM of ABTS, respectively.

Using the 'activity-on-plate' high-throughput assay screening a mutant library of 25,000 variants was screened (figure 3.13). All clones that presented higher activity than wild-type (153 variants), as measured by the intensity of the purple colour in the Whatman paper, were selected for rescreening (figure 3.14). Seven variants were chosen and a new round of rescreening was performed (figure 3.15). A large variation in activity was observed among colonies of the same variant and as a consequence, the rescreening of the best seven mutants was performed in 96-deep well plates.

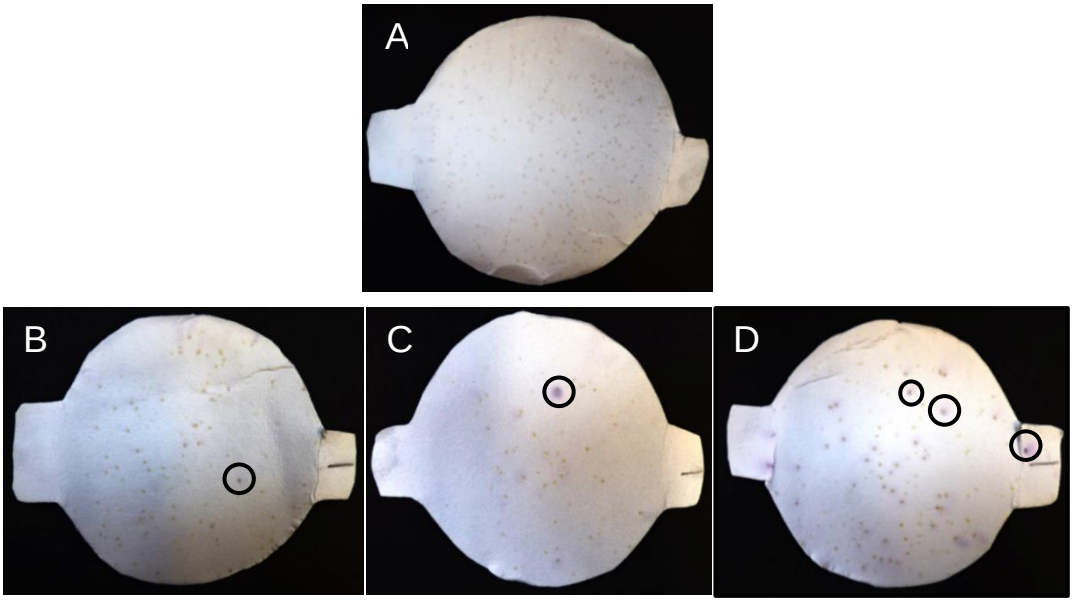

Figure 3.13 'Activity-on-plate' high-throughput assay (10 U HRP, 1 mM ABTS and 10 mM D-glucose) using BL21 star cells expressing (A) wild-type *asP2Ox* gene and (B-D) mutant library constructed using epPCR in the presence of 0.01 mM $MnCl_2$. Colonies within circles represent variants with improved activity visible by the darker colour.

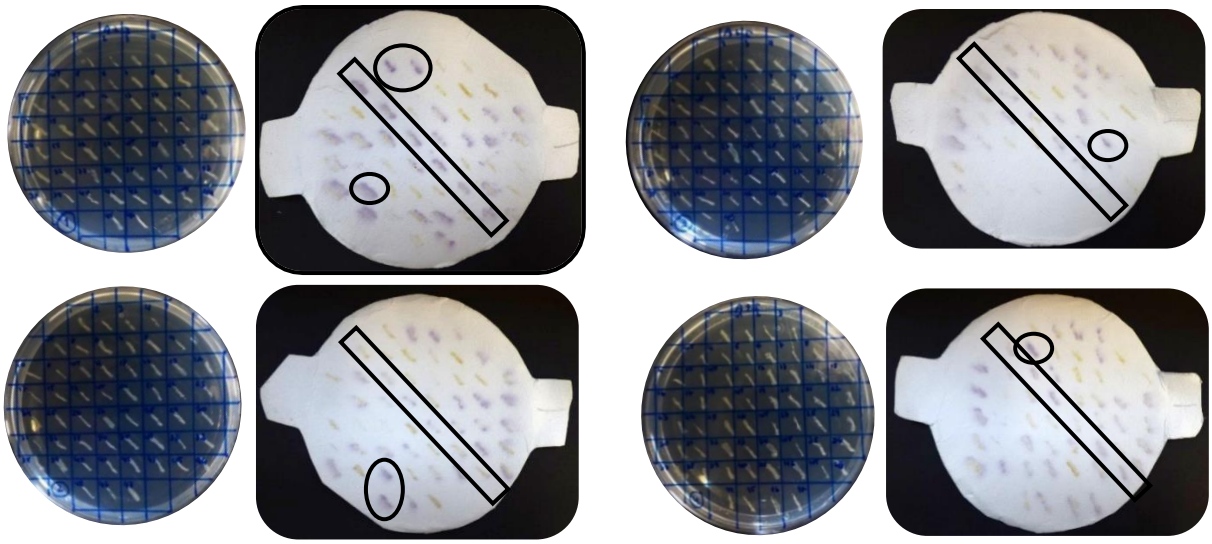

Figure 3.14 Rescreening using the same conditions than previously used of the best 153 variants through 'activity-on-plate'. The seven clones showing a faster and stronger purple colour than wild-type were chosen for a new rescreening. Colonies within circles represent variants with improved activity and inside rectangles are represented colonies overexpressing wild-type *asP2Ox*.

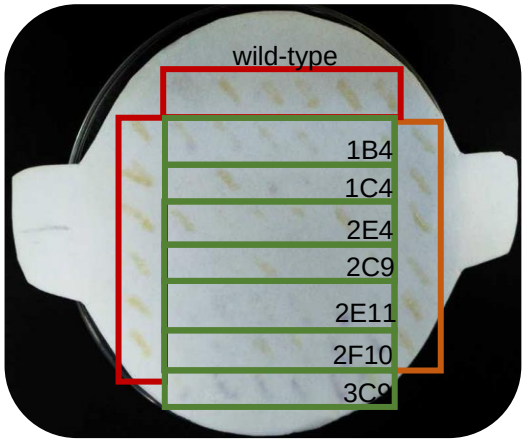

Figure 3.15 Rescreening of the best seven variants through 'activity-on-plate'. The wild-type AsP2Ox and variants have shown different growth rates and consequently very weak or inexistence activity.

Growing the cells harbouring the wild-type *asP2Ox* gene in 96-deep well plates led to similar values of final OD_{600nm} (1.3 ± 0.3) with a lower coefficient of variation as compared with the standard 96 well-plates (23% in 96 deep well-plates and 33% in standard 96 well-plates) and approximately 4-times higher total protein concentration (2.2 mg/mL ± 0.1) with a lower coefficient of variation (5% in 96-deep well plates and 33% in standard 96 well-plates). Consequently, the seven variants were grown in 96-deep well plates and only the 2C9 variant showed a very weak green colour comparing with control (figure 3.16) and a specific activity of 0.7 nmol/min.mg was measured.

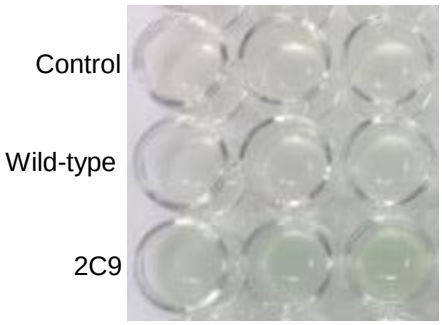

Figure 3.16 Enzymatic activity using crude extracts of wild-type AsP2Ox and 2C9 in the presence of 100 mM D-glucose, 10 U HRP and 1 mM ABTS in 100 mM sodium phosphate buffer at pH 6.5. In the control reaction no crude extract was added.

Based on these results, 2C9 plasmid was extracted, transformed on DH5-α cloning strain, purified and sent to sequencing. The results showed that 2C9 has three nucleotide alterations that led to two amino acid substitutions and a silent mutation (A35T, F300V and Q343Q). In order to evaluate the performance of the 2C9 hit and to compare with wild-type AsP2Ox, it was decided to first characterize the enzyme before going forward to a second generation of evolution.

3.4. Kinetic and biochemical characterization of the hit 2C9 variant

3.4.1 Structural analysis of mutations that improved the activity of 2C9

As previously mentioned, the 2C9 hit accumulated two non-synonymous (A35T and F300V) and one synonymous mutation (Q343Q). Through the analyses of a model structure of AsP2Ox constructed based on the crystal structure of pyranose 2-oxidase from *P. chrysosporium* (PDB code: 4MIG) provided by Prof Willem van Berkel (figure 3.17), it is possible to observe that the mutation A35T is located in a loop that belongs to the Rossmann domain of FAD-binding subdomain. This mutation is located about 20 Å from the FAD cofactor and the catalytic residues His440 and Asn482. In *T. multicolor* and *Peniophora sp.*, a tyrosine residue is present in the correspondent position unlike *P. chrysosporium* that presents a leucine amino acid residue. The other amino acid substitution present in 2C9 is F300V that is located in a β-sheet of the substrate-binding domain and is about 15 Å from the FAD cofactor and the catalytic residues His440 and Asn482 (figure 3.17). A phenylalanine, that is an aromatic and hydrophobic residue, was substituted by the smaller valine (hydrophobic) amino acid. In *T. multicolor*, *Peniophora sp.*, and *P. chrysosporium*, a cysteine which is a hydrophilic residue is present in the corresponding position.

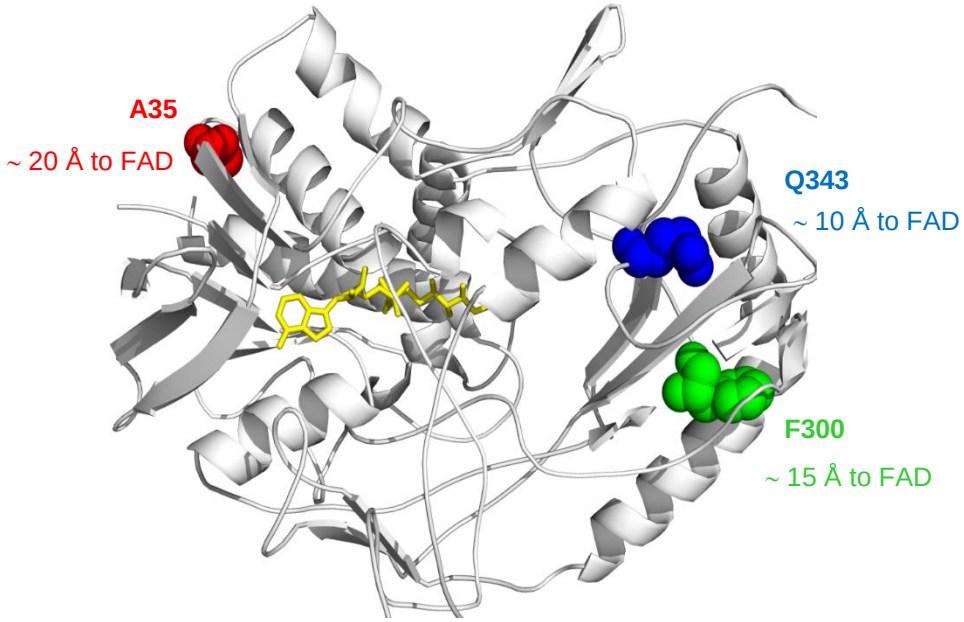

Figure 3.17 Model structure of wild-type AsP2Ox where the FAD cofactor is represented in yellow sticks. A35 is in red, F300 in green and Q343 in blue colour. The distances from A35, F300V and Q343 to the FAD cofactor are represented in blue in Ångström (Å).

3.4.2 Spectroscopic analysis and identification of FAD ligation

After the production and purification of the protein 2C9 in the same conditions of wild-type AsP2Ox, it was possible to observe that despite the similar final OD_{600nm} of cell cultures (3.9 and 4.4 for wild-type and 2C9, respectively), the concentration of purified protein was 3-fold lower for 2C9 when compared with wild-type AsP2Ox (20 and 6 mg protein per L of LB media, respectively; figure 3.18).

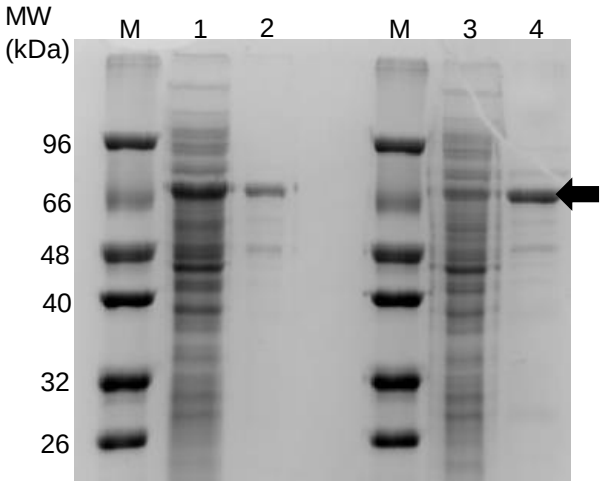

Figure 3.18 SDS-PAGE of BL21 star crude extracts overproducing wild-type and 2C9 purified proteins. (M) Marker, (1) crude extracts of cells overproducing wild-type AsP2Ox protein, (2) AsP2Ox after purification using a metal affinity chromatography, (3) crude extracts of cells overproducing 2C9 variant protein and (4) 2C9 after purification using a metal affinity chromatography. The arrow indicates the band that corresponds to AsP2Ox proteins (~64 kDa).

The UV-Vis absorption spectra of two different eluted purified fractions from the metal affinity chromatography column were recorded and compared with the UV-Vis absorption spectrum of wild-type AsP2Ox (figure 3.19-A). Despite the purified 2C9 fractions showing the characteristic yellow colour of flavins, the UV-Vis absorption spectrum of one of the fractions just presented one band with absorbance maximum at 405 nm that corresponds to fully-reduced neutral flavin $FADH_2$ (dashed line) while the UV-Vis spectrum of the second fraction, in addition to the 405 nm band presented an additional absorbance peak at 340 nm that corresponds to fully-reduced anionic flavin $FADH^-$ (dotted line)[71,72]. It is possible to conclude that performing cell disruption and purification of the hit 2C9 in the presence of light, led to the photoreduction of FAD cofactor which consequently become inactive. These results demonstrate a higher sensitivity of 2C9 to light inactivation as compared to the wild-type enzyme. Therefore, cell disruption and purification of the variant enzyme was performed in the total absence of light and a UV-Vis absorption spectrum of the purified enzyme was recorded (figure 3.19-B). When 2C9 was purified in dark conditions, the UV-Vis absorption spectrum of AsP2Ox exhibited the two typical absorbance maxima at 390 and 460 nm. The treatment of the enzyme with 5% TCA resulted in a colourless pellet and a yellow supernatant displaying the characteristic FAD absorbance spectrum, and indicating that the flavin cofactor is not covalently bonded to the 2C9 enzyme similarly to the wild-type enzyme as assessed by a down-shift of both absorbance maxima to 380 and 450 nm after protein denaturation[67] (dotted line). However, no activity could be measured using this purified protein most likely due to photoreduction and inactivation during the procedures to measure enzymatic activity.

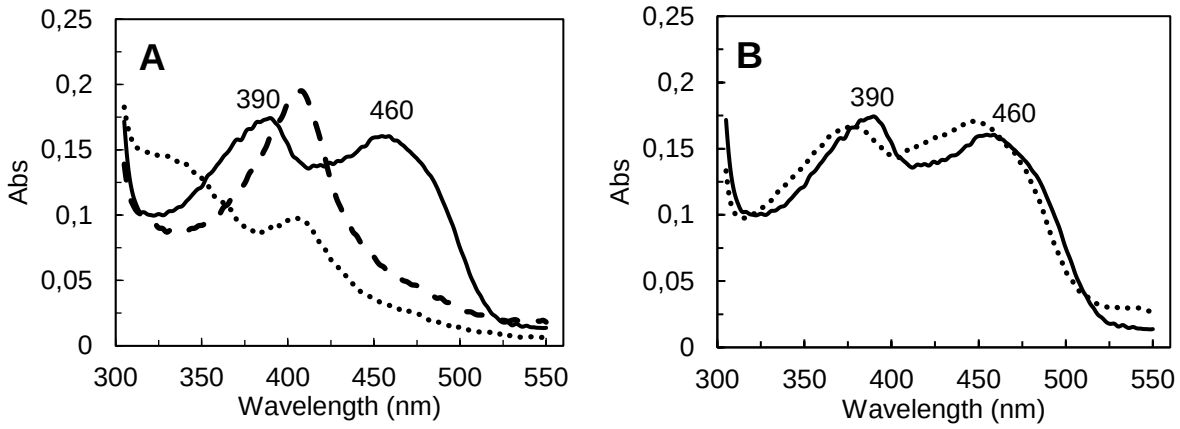

Figure 3.19 (A) UV-vis spectra of AsP2Ox as isolated (solid line) and of 2C9 fractions after purification (dashed and dotted lines) (B) UV-vis spectra of purified 2C9 as isolated (solid line) and after treatment with 0.4% (w/v) SDS or 5%TCA followed by heating and centrifugation (dotted line).

3.5 Site-directed mutagenesis

In order to identify the role of mutations on the enzyme variant properties, including the lower production yields and the photo inactivation of the FAD cofactor, responsible for the absence of activity in purified 2C9, three variant enzymes were constructed using site-directed mutagenesis: A35T, F300V and the double variant 2C9* (A35T/F300V). The five proteins (wild-type, 2C9, 2C9*, A35T and F300V) were first overproduced in a small scale culture of 100 mL to analyse their differences in protein production. The SDS-PAGE showed that crude extracts of variant proteins presented lower production yields than wild-type (figure 3.20). However, the production of 2C9 is significantly increased when the silent mutation was removed (2C9*). Despite synonymous mutations do not affect the identity of the encoded amino acid, each organism has a preference for a set of codons over others (codon bias) and its different utilization can directly affect the protein expression levels and regulation and the protein folding[73]. The silent mutation present in the 2C9 hit (Q343Q) leads to around half of tRNA gene copy numbers in *E.coli* when compared with the wild-type nucleotide[73] and is at least partially responsible for the lower expression of 2C9 when compared with the wild-type enzyme.

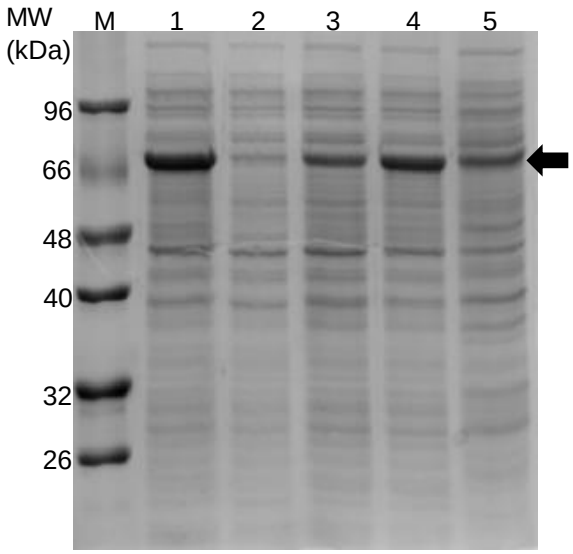

Figure 3.20 SDS-PAGE of BL21 star crude extracts overproducing wild-type and mutant proteins. (M) Marker, crude extracts overproducing (1) wild-type, (2) 2C9, (3) 2C9*, (4) A35T and (5) F300V proteins. The arrow indicates the band that corresponds to AsP2Ox proteins (~64 kDa).

Large scale cultures (1L) of BL21 star overproducing wild-type, 2C9*, A35T and F300V proteins were performed with the objective of purifying and characterizing the variants. The results confirmed the higher protein yields in wild-type and A35T proteins as compared to 2C9* and F300V variants (table 3.5). Therefore, it was possible to conclude that both the silent Q343Q and F300V mutations are responsible for the lower expression of 2C9* by *E.coli* cells. The 2C9* variant without the silent mutation had a production yield 2-fold higher when compared with the 2C9 variant. Furthermore, 2C9* (without the silent mutation) showed 3-fold higher specific activity. Interestingly, both single variants showed lower activity than 2C9* showing that the activity of this variant is dependent on the simultaneous presence of both mutations (table 3.5).

Table 3.5 Total protein concentration achieved from 1L of culture of Bl21 star cells producing wild-type, 2C9, 2C9*, A35T and F300V proteins determined after purification using a metal affinity chromatography and specific activity achieved after enzymatic assays at 37ºC, in 100 mM sodium phosphate buffer at pH 6.5 in the presence of 1 M D-glucose, 1 mM ABTS and 10 U HRP.

AsP2Ox protein	$[Protein]_{total}$ (mg)	Specific Activity (nmol/min.mg)
Wild-type	39 ± 1.8	1.5 ± 0.03
2C9	6 ± 0.4	-
2C9*	12 ± 1.4	4.8 ± 0.34
A35T	32 ± 1.0	1.1 ± 0.03
F300V	12 ± 0.4	2.4 ± 0.10

After purification in the presence of light and confirmation of the purity of the proteins through a SDS-PAGE (data not shown), UV-Vis absorption spectra were recorded before and after treatment with 0.4% (w/v) SDS where it was possible to observe that variants 2C9*, A35T and F300V presented the typical UV-vis absorption spectra, with two absorbance maxima at 390 and 460 nm, and that the FAD cofactor is non-covalently associated (figure 3.21). These results showed that the silent mutation Q343Q, present in 2C9 hit close to the FAD cofactor (*ca.* 10Å-figure 3.17), is the responsible for the photo-inactivation behaviour of 2C9 hit variant. Silent single nucleotide polymorphisms have been assumed to have no effect on gene function or phenotype due to the inexistence of amino acid change of the protein product. However, in recent studies it was verified that synonymous codon substitutions can alter the translation kinetics of a determined mRNA due to the fact that infrequent codons in mRNA appear to be slowly translated, whereas frequent codons are rapidly translated with consequences in the protein folding that can result in different conformations and functions, for example, an altered substrate specificity[74,75] or as in the present case, a likely conformation that results in the spontaneous formation of reduced FAD intermediates in the presence of light.

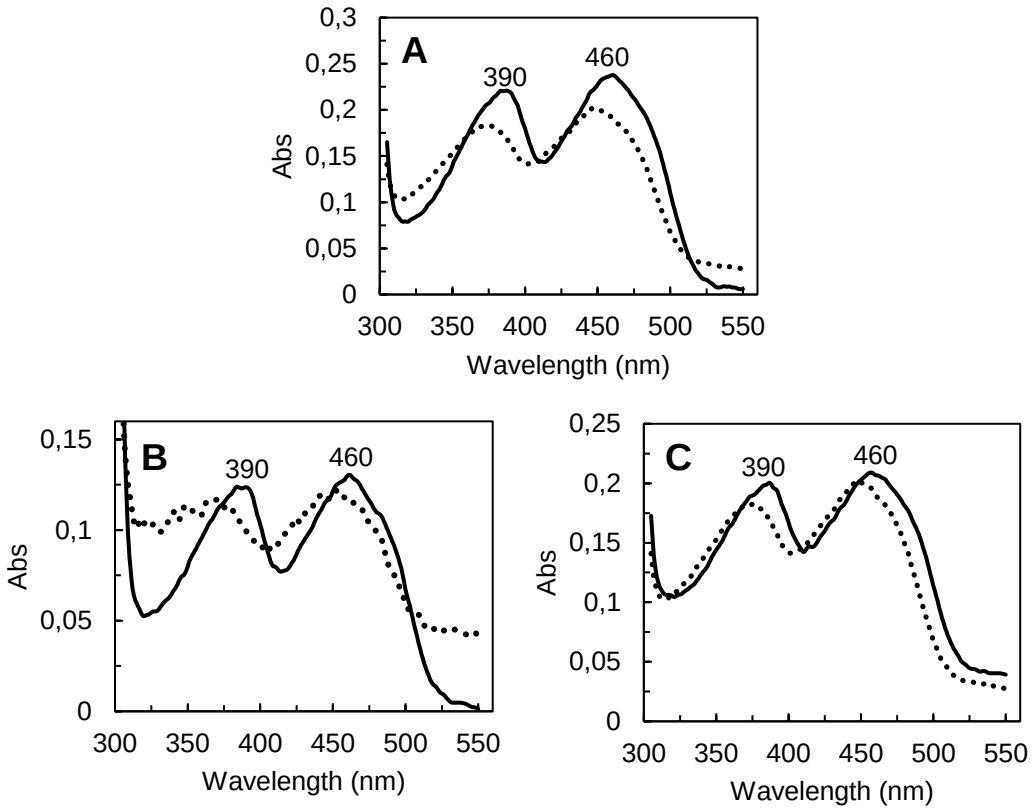

Figure 3.21 UV-vis spectra of (A) 2C9*, (B) A35T and (C) F300V as isolated (solid line) and after treatment with 0.4% (w/v) SDS (dotted line).

Steady-state kinetic analyses were performed with wild-type and variant enzymes using D-glucose and O_2 (figure 3.22). The A35T enzyme presents a similar relation of specific activity vs. substrate concentration to the wild-type and obtained data could be fitted using the Michaelis-Menten equation. However, for 2C9* and F300V enzymes it was evident that enzyme rates achieved a maximum at approximately 1 M of D-glucose and after that concentration decline as the substrate concentration increased. The sharp decrease in rates impaired fitting the data to a substrate inhibition curve. Therefore, only the data up to 1.2 M was considered and fit using the Michaelis-Menten equation. The apparent steady-state kinetic parameters in table 3.6 shows that the hit 2C9* presents a 3-fold higher enhanced efficiency (k_{cat}/K_m) to the wild-type enzyme. Moreover, it is also possible to observe that apparently A35T is a neutral mutation, with similar k_{cat} and K_m to wild type, while F300V is a functional mutation that becomes more beneficial when combined with A35T, considering that 2C9* exhibited a higher k_{cat}/K_m than the single F300V variant (table 3.6), a phenomenon designated by positive epistasis[76]. Nevertheless the catalytic efficiency of 2C9* is still six orders of magnitude lower when compared with P2Ox characterized from fungal origins[11,12] and multiple rounds of directed evolution are needed to improve its efficiency.

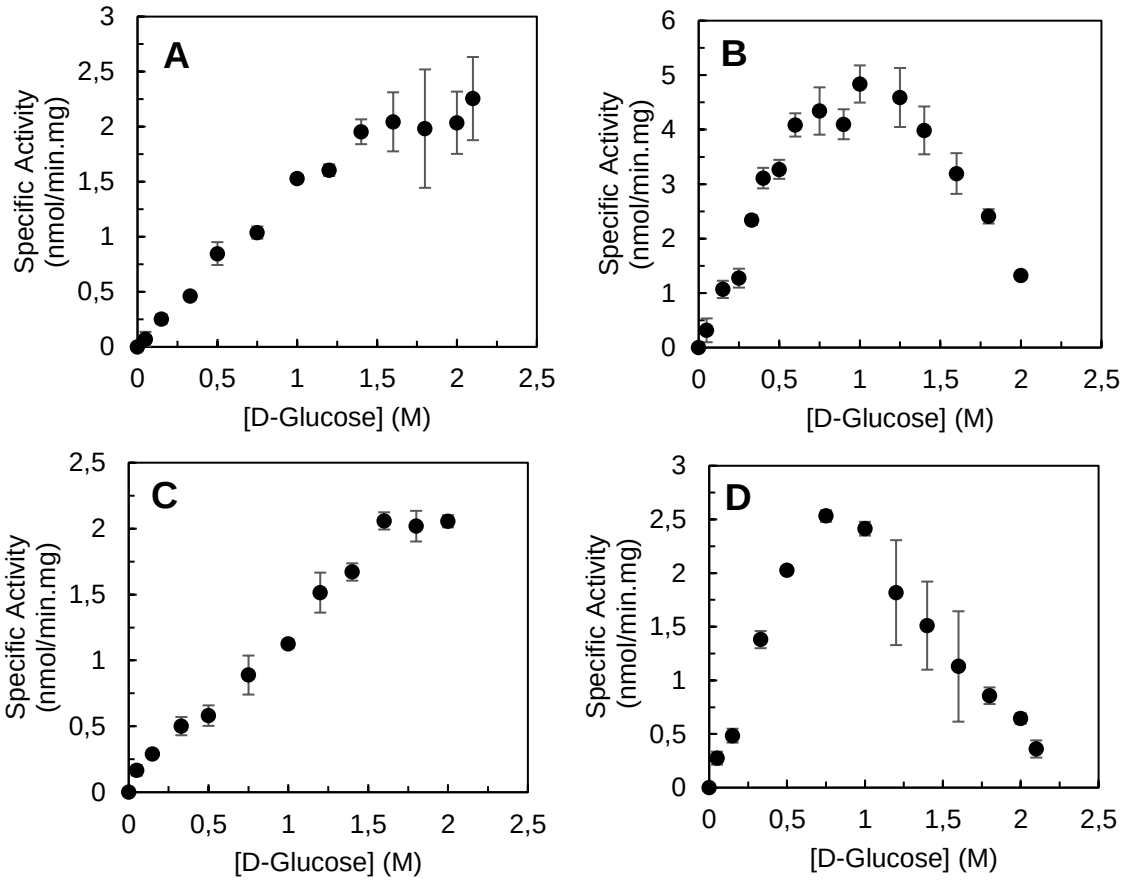

Figure 3.22 Apparent steady-state kinetic analysis of (A) wild-type, (B) 2C9*, (C) A35T and (D) F300V proteins for D-glucose using O_2 as electron acceptor. Reactions were performed in 100 mM sodium phosphate buffer at pH 6.5, using O_2 saturated solutions at 37°C, and the ABTS-peroxidase assay. The kinetic parameters were fitted directly using the Michaelis-Menten equation (Origin-Lab software).

Table 3.6 Apparent steady-state kinetic parameters of AsP2Ox (wild-type and variants) determined using D-glucose and O_2. Enzymatic assays were performed at 37ºC, in 100 mM sodium phosphate buffer at pH 6.5 in the presence of 1 M D-glucose, 1 mM ABTS and 10 U HRP.

Protein	K_m (M)	V_{max} (nmol/min.mg)	k_{cat} (s^{-1})	k_{cat}/K_m ($M^{-1}s^{-1}$)
Wild-type	0.7 ± 0.04	2.2 ± 0.4	0.002 ± 0.0002	0.003 ± 0.001
2C9*	0.5 ± 0.06	6.0 ± 1.6	0.005 ± 0.001	0.010 ± 0.01
A35T	0.7 ± 0.14	2.3 ± 0.4	0.002 ± 0.0003	0.003 ± 0
F300V	0.4 ± 0.04	3.4 ± 0.3	0.003 ± 0.0003	0.007 ± 0

Overall results show that the most appropriate candidate to be used as parent in the second generation of directed evolution is 2C9* since the elimination of the silent mutation improved the stability as well as the production of the enzyme as compared to variant 2C9.

4. Conclusions

This work was targeted at improving the kinetic properties of AsP2Ox through protein engineering. The development of an effective and simple strategy of evolution that allowed finding and identifying improved variants from a library of thousands of mutants was performed. In spite of the difficulties encountered in all steps of validation of the directed evolution approach it was possible to develop a solid strategy through the use of epPCR at a low concentration of $MnCl_2$ (0.01 mM) and an 'activity-on-plate' screening based on a coupled HRP-ABTS colorimetric assay. The implementation of the validated strategy allowed testing a high number of variants (25 000) with an appropriate mutation rate (1-3 nucleotide base substitutions per gene) to an increased oxidase activity in a short period of time. The hit variant (2C9) was identified after the first generation of evolution, showing three mutations located at the surface of the protein. The utilization of a complementary strategy of site-directed mutagenesis unveiled the effect of each mutation present in the variant enzyme and allowed to select the best candidate to be used in the second generation of directed evolution.

In the future, the Microbial and Enzyme Technology laboratory is particularly interested in establishing collaborations for the application of improved AsP2Ox variants in biosensors to control the sugar levels in patients with diabetes through the use of cellulose fiber paper. It is also a purpose to study the structure-function relationship determinants for the activity and stability of AsP2Ox, contributing with new fundamental knowledge on P2Oxs features and contributing to answer the long-standing question in protein science of "how function and structure are related". Considering, this goal two collaborations were established, with the group of Prof Willem van Berkel (Wageningen University), a worldwide reference in the field of flavoproteins and with Dr. Carlos Frazão, head of the Structural Biology laboratory at ITQB, an experienced crystallographer with a high publication track record, to determine the crystal structure of wild-type AsP2Ox which hopefully will be followed by the determination of the structure of variant enzymes found in the course of evolution. Finally, we aim at investigating the molecular mechanisms of enzyme fitness evolution, a critical knowledge for engineering new proteins, metabolic pathways and organisms for biotechnological applications.

5. Bibliography

1. Wongnate, T. & Chaiyen, P. The substrate oxidation mechanism of pyranose 2-oxidase and other related enzymes in the glucose-methanol-choline superfamily. *FEBS J.* **280,** 3009–3027 (2013).
2. Giffhorn, F. Fungal pyranose oxidases: Occurrence, properties and biotechnical applications in carbohydrate chemistry. *Appl. Microbiol. Biotechnol.* **54,** 727–740 (2000).
3. Mendes, S. *et al.* Characterization of a bacterial pyranose 2-oxidase from Arthrobacter siccitolerans. *J. Mol. Catal. B Enzym.* (2016). doi:10.1016/j.molcatb.2016.11.005
4. Dietrich, D. & Crooks, C. Gene cloning and heterologous expression of pyranose 2-oxidase from the brown-rot fungus, Gloeophyllum trabeum. *Biotechnol. Lett.* **31,** 1223–1228 (2009).
5. Takakura, Y. & Kuwata, S. Purification, characterization, and molecular cloning of a pyranose oxidase from the fruit body of the basidiomycete, Tricholoma matsutake. *Biosci. Biotechnol. Biochem.* **67,** 2598–2607 (2003).
6. Danneel, H.-J., Rössner, E., Zeeck, A. & Giffhorn, F. Purification and characterization of a pyranose oxidase from the basidiomycete Peniophora gigantea and chemical analyses of its reaction products. **802,** 795–802 (1993).
7. Pisanelli, I. *et al.* Pyranose 2-oxidase from Phanerochaete chrysosporium-Expression in E. coli and biochemical characterization. *J. Biotechnol.* **142,** 97–106 (2009).
8. Tan, T. C., Haltrich, D. & Divne, C. Regioselective control of β-d-glucose oxidation by pyranose 2-oxidase is intimately coupled to conformational degeneracy. *J. Mol. Biol.* **409,** 588–600 (2011).
9. Kujawa, M. *et al.* Structural basis for substrate binding and regioselective oxidation of monosaccharides at C3 by pyranose 2-oxidase. *J. Biol. Chem.* **281,** 35104–35115 (2006).
10. Hassan, N. *et al.* Crystal structures of Phanerochaete chrysosporium pyranose 2-oxidase suggest that the N-terminus acts as a propeptide that assists in homotetramer assembly. *FEBS Open Bio* **3,** 496–504 (2013).
11. Salaheddin, C. *et al.* Characterisation of recombinant pyranose oxidase from the cultivated mycorrhizal basidiomycete Lyophyllum shimeji (hon-shimeji). *Microb. Cell Fact.* **9,** 57 (2010).
12. Leitner, C., Volc, J. & Haltrich, D. Purification and Characterization of Pyranose Oxidase from the White Rot Fungus Trametes multicolor Purification and Characterization of Pyranose Oxidase from the White Rot Fungus Trametes multicolor. **67,** 3636–3644 (2001).
13. Leitner, C., Haltrich, D., Nidetzky, B., Prillinger, H. & Kulbe, K. D. Production of a novel pyranose 2-oxidase by basidiomycete Trametes multicolor. *Appl. Biochem. Biotechnol.* **70–72,** 237–48 (1998).
14. Sørensen, H. P. & Mortensen, K. K. Soluble expression of recombinant proteins in the cytoplasm of Escherichia coli. *Microb. Cell Fact.* **4,** 1 (2005).
15. Qin, S., Li, W. J., Dastager, S. G. & Hozzein, W. N. Editorial: Actinobacteria in special and extreme habitats: Diversity, function roles, and environmental adaptations. *Front. Microbiol.* **7,** 1–2 (2016).
16. Shivlata, L. & Satyanarayana, T. Thermophilic and alkaliphilic Actinobacteria: Biology and potential applications. *Front. Microbiol.* **6,** 1–29 (2015).
17. Santacruz-Calvo, L., González-López, J. & Manzanera, M. Arthrobacter siccitolerans sp. nov., a highly desiccation-tolerant, xeroprotectant-producing strain isolated from dry soil. *Int. J. Syst. Evol. Microbiol.* **63,** 4174–4180 (2013).
18. Manzanera, M., Vílchez, J. I. & Calvo, C. Genome sequence of Arthrobacter siccitolerans 4J27, a xeroprotectant-producing desiccation-tolerant microorganism. *Genome Announc.* **2,** 14–15 (2014).
19. Martin Hallberg, B., Leitner, C., Haltrich, D. & Divne, C. Crystal structure of the 270 kDa homotetrameric lignin-degrading enzyme pyranose 2-oxidase. *J. Mol. Biol.* **341,** 781–796 (2004).
20. Bannwarth, M., Bastian, S., Heckmann-Pohl, D., Giffhorn, F. & Schulz, G. E. Crystal structure of

pyranose 2-oxidase from the white-rot fungus Peniophora sp. *Biochemistry* **43,** 11683–11690 (2004).

21. Halada, P., Leitner, C., Sedmera, P., Haltrich, D. & Volc, J. Identification of the covalent flavin adenine dinucleotide-binding region in pyranose 2-oxidase from Trametes multicolor. *Anal. Biochem.* **314,** 235–242 (2003).

22. Spadiut, O., Tan, T. C., Pisanelli, I., Haltrich, D. & Divne, C. Importance of the gating segment in the substrate-recognition loop of pyranose 2-oxidase. *FEBS J.* **277,** 2892–2909 (2010).

23. Tan, T. C. *et al.* H-bonding and positive charge at the N(5)/O(4) locus are critical for covalent flavin attachment in Trametes pyranose 2-oxidase. *J. Mol. Biol.* **402,** 578–594 (2010).

24. Pitsawong, W. *et al.* A conserved active-site threonine is important for both sugar and flavin oxidations of pyranose 2-oxidase. *J. Biol. Chem.* **285,** 9697–9705 (2010).

25. Sucharitakul, J., Wongnate, T. & Chaiyen, P. Kinetic isotope effects on the noncovalent flavin mutant protein of pyranose 2-oxidase reveal insights into the flavin reduction mechanism. *Biochemistry* **49,** 3753–3765 (2010).

26. Artolozaga, M. J., Kubátová, E., Volc, J. & Kalisz, H. M. Pyranose 2-oxidase from Phanerochaete chrysosporium - Further biochemical characterisation. *Appl. Microbiol. Biotechnol.* **47,** 508–514 (1997).

27. Adamson, T. L., Cook, C. B. & LaBelle, J. T. Detection of 1,5-Anhydroglucitol by Electrochemical Impedance Spectroscopy. *J. Diabetes Sci. Technol.* **8,** 350–355 (2014).

28. Jing, F. *et al.* A novel fully enzymatic method for determining glucose and 1,5-anhydro-d-glucitol in serum of one cuvette. *Appl. Biochem. Biotechnol.* **150,** 327–335 (2008).

29. Dungan, K. M. 1,5-anhydroglucitol (GlycoMark) as a marker of short-term glycemic control and glycemic excursions. *Expert Rev. Mol. Diagn.* **8,** 9–19 (2008).

30. Kim, J. H. *et al.* Enzyme precipitate coating of pyranose oxidase on carbon nanotubes and their electrochemical applications. *Biosens. Bioelectron.* **87,** 365–372 (2017).

31. ODACI DEMIRKOL, D., OZDEMIR, C., PILLOTON, R. & TIMUR, S. Carbon Nanotube Modified Screen Printed Electrodes: Pyranose Oxidase Immobilization Platform for Amperometric Enzyme Sensors. *Süleyman Demirel Üniversitesi Fen Bilim. Enstitüsü Derg.* **21,** 286 (2017).

32. Giffhorn, F., Köpper, S., Huwig, A. & Freimund, S. Rare sugars and sugar-based synthons by chemo-enzymatic synthesis. *Enzyme Microb. Technol.* **27,** 734–742 (2000).

33. Freimund, S., Huwig, A., Giffhorn, F. & Köpper, S. Rare keto-aldoses from enzymatic oxidation: Substrates and oxidation products of pyranose 2-oxidase. *Chem. - A Eur. J.* **4,** 2442–2455 (1998).

34. Freimund, S., Baldes, L., Huwig, A. & Giffhorn, F. Enzymatic synthesis of D-glucosone 6-phosphate (D-arabino-hexos-2-ulose 6-(dihydrogen phosphate)) and NMR analysis of its isomeric forms. *Carbohydr. Res.* **337,** 1585–1587 (2002).

35. Gabriel, J. Short Communication High-performance liquid chromatographic the antibiotic cortalcerone. **542,** 3–6 (1991).

36. Koths, K., Halenbeck, R. & Moreland, M. Synthesis of the antibiotic cortalcerone from d-glucose using pyranose 2-oxidase and a novel fungal enzyme, aldos-2-ulose dehydratase. *Carbohydr. Res.* **232,** 59–75 (1992).

37. D, H. *et al.* A Convenient Enzymatic Procedure for the Production of Aldose-Free D -Tagatose a. *Ann. N. Y. Acad. Sci.* **864,** 295–299 (1998).

38. Plumeré, N., Henig, J. & Campbell, W. H. Enzyme-Catalyzed O(2) Removal System for Electrochemical Analysis under Ambient Air: Application in an Amperommetric Nitrate Biosensor. *Anal. Chem.* **49945,** 1–13 (2012).

39. Swoboda, M. *et al.* Enzymatic Oxygen Scavenging for Photostability without pH Drop in. **1,** 6364–6369 (2012).

40. Leemhuis, H., Kelly, R. M. & Dijkhuizen, L. Directed evolution of enzymes: Library screening strategies. *IUBMB Life* **61,** 222–228 (2009).

41. Lane, M. D. & Seelig, B. Advances in the directed evolution of proteins. *Curr. Opin. Chem. Biol.* **22,** 129–136 (2014).

42. Turanli-yildiz, B., Alkim, C. & Cakar, Z. P. Protein Engineering Methods and Applications. *Protein Eng.* 33–58 (2012). doi:10.5772/27306

43. Chen, R. Enzyme engineering: Rational redesign versus directed evolution. *Trends Biotechnol.* **19,** 13–14 (2001).

44. Antikainen, N. M. & Martin, S. F. Altering protein specificity: Techniques and applications. *Bioorganic Med. Chem.* **13,** 2701–2716 (2005).

45. Nixon, A. E. & Firestine, S. M. Rational and 'irrational' design of proteins and their use in biotechnology. *IUBMB Life* **49,** 181–7 (2000).

46. Williams, G. J., Nelson, A. S. & Berry, A. Directed evolution of enzymes for biocatalysis and the life sciences. *Cell. Mol. Life Sci.* **61,** 3034–3046 (2004).

47. Bloom, J. D. *et al.* Evolving strategies for enzyme engineering. *Curr. Opin. Struct. Biol.* **15,** 447–452 (2005).

48. Nishikawa, T., Sunami, T., Matsuura, T. & Yomo, T. Directed evolution of proteins through in vitro protein synthesis in liposomes. *J. Nucleic Acids* **2012,** (2012).

49. Packer, M. S. & Liu, D. R. Methods for the directed evolution of proteins. *Nat. Rev. Genet.* **16,** 379–394 (2015).

50. Xiao, H., Bao, Z. & Zhao, H. High throughput screening and selection methods for directed enzyme evolution. *Ind. Eng. Chem. Res.* **54,** 4011–4020 (2015).

51. Cirino, P. C., Mayer, K. M. & Umeno, D. Generating mutant libraries using error-prone PCR. *Methods Mol. Biol.* **231,** 3–9 (2003).

52. Mccullum, E. O., Williams, B. a R., Zhang, J. & Chaput, J. C. In Vitro Mutagenesis Protocols. *Methods Mol. Biol.* **634,** 103–109 (2010).

53. Cobb, R. E., Chao, R. & Zhao, H. Directed Evolution: Past, Present and Future. *AIChE J.* **59,** 1432–1440 (2013).

54. Kikuchi, M. & Harayama, S. DNA shuffling and family shuffling for in vitro gene evolution. *Methods Mol. Biol.* **182,** 243–57 (2002).

55. Brakmann, S. Discovery of superior enzymes by directed molecular evolution. *ChemBioChem* **2,** 865–871 (2001).

56. Siloto, R. M. P. & Weselake, R. J. Site saturation mutagenesis: Methods and applications in protein engineering. *Biocatal. Agric. Biotechnol.* **1,** 181–189 (2012).

57. Georgescu, R., Bandara, G. & Sun, L. Saturation mutagenesis. *Methods Mol. Biol.* **231,** 75–83 (2003).

58. Chronopoulou, E. G. & Labrou, N. E. Site-saturation mutagenesis: A powerful tool for structure-based design of combinatorial mutation libraries. *Curr. Protoc. Protein Sci.* 1–10 (2011). doi:10.1002/0471140864.ps2606s63

59. Yang, G. & Withers, S. G. Ultrahigh-throughput FACS-based screening for directed enzyme evolution. *ChemBioChem* **10,** 2704–2715 (2009).

60. Olsen, M. J., Gam, J., Iverson, B. L. & Georgiou, G. High-throughput FACS method for directed evolution of substrate specificity. *Methods Mol. Biol. Then Totowa-* **230,** 329–342 (2003).

61. Belousov, V. V *et al.* Genetically encoded fluorescent indicator for intracellular hydrogen peroxide. *Nat. Methods* **3,** 281–286 (2006).

62. Lim, J. B. & Sikes, H. D. Use of a genetically encoded hydrogen peroxide sensor for whole cell screening of enzyme activity. *Protein Eng. Des. Sel.* **28,** 79–83 (2015).

63. Nguyen, V. D. *et al.* Pre-expression of a sulfhydryl oxidase significantly increases the yields of eukaryotic disulfide bond containing proteins expressed in the cytoplasm of E.coli. *Microb. Cell Fact.* **10,** 1 (2011).

64. Bradford, M. M. A rapid and sensitive method for the quantitation of microgram quantities of protein utilizing the principle of protein-dye binding. *Anal. Biochem.* **72,** 248–254 (1976).

65. Danneel, H. J., Ullrich, M. & Giffhorn, F. Goal-oriented screening method for carbohydrate oxidases produced by filamentous fungi. *Enzyme Microb. Technol.* **14,** 898–903 (1992).

66. Brissos, V., Ferreira, M., Grass, G. & Martins, L. O. Turning a Hyperthermostable Metallo-Oxidase into a Laccase by Directed Evolution. *ACS Catal.* **5,** 4932–4941 (2015).

67. Aliverti, a, Curti, B. & Vanoni, M. a. Identifying and quantitating FAD and FMN in simple and in iron-sulfur-containing flavoproteins. *Methods Mol. Biol.* **131,** 9–23 (1999).

68. Salazar, O. & Sun, L. Evaluating a screen and analysis of mutant libraries. *Methods Mol. Biol.* **230,** 85–97 (2003).

69. Johnson, B. H. & Hecht, M. H. Recombinant proteins can be isolated from E. coli cells by repeated cycles of freezing and thawing. *Bio/technology (Nature Publishing Company)* **12,** 1357–1360 (1994).

70. Bourbonnais, R., Leech, D. & Paice, M. G. Electrochemical analysis of the interactions of laccase mediators with lignin model compounds. *Biochim. Biophys. Acta* **1379,** 381–390 (1998).

71. Kao, Y. T. *et al.* Ultrafast dynamics of flavins in five redox states. *J. Am. Chem. Soc.* **130,** 13132–13139 (2008).

72. Zhao, R.-K. *et al.* Ultrafast transient mid IR to visible spectroscopy of fully reduced flavins. *Phys. Chem. Chem. Phys.* **13,** 17642 (2011).

73. Quax, T. E. F., Claassens, N. J., Oost, J. Van Der & Haven, N. Codon Bias as a Means to Fine-Tune Gene Expression. *Mol Cell* **59,** 149–161 (2016).

74. Komar, A. A. SNPs, Silent But Not Invisible. *Science (80-.).* **315,** 466–467 (2007).

75. Cortazzo, P. *et al.* Silent mutations affect in vivo protein folding in Escherichia coli. *Biochem. Biophys. Res. Commun.* **293,** 537–541 (2002).

76. Miton, C. M. & Tokuriki, N. How mutational epistasis impairs predictability in protein evolution and design. *Protein Sci.* **25,** 1260–1272 (2016).